AD-A274 897

②

NAVAL POSTGRADUATE SCHOOL
Monterey, California

DTIC
S ELECTE
JAN 2 5 1994
C D

THESIS

CODE DIVISION MULTIPLE ACCESS LOCAL AREA
NETWORK COMMUNICATIONS EMPLOYING
FIBER OPTIC SIGNAL PROCESSING
TECHNIQUES

by

Bruce A. Legge

September, 1993

Thesis Advisor: John P. Powers

94-02050

94 1 24 061

REPORT DOCUMENTATION PAGE

Form Approved
OMB No 0704-0188

1. AGENCY USE ONLY (Leave blank)	2. REPORT DATE September 1993	3. REPORT TYPE AND DATES COVERED Master's Thesis

4. TITLE AND SUBTITLE CODE DIVISION MULTIPLE ACCESS LOCAL AREA NETWORK COMMUNICATIONS EMPLOYING FIBER OPTIC SIGNAL PROCESSING TECHNIQUES

5. FUNDING NUMBERS

6. AUTHOR(S)

Legge, Bruce Allen

7. PERFORMING ORGANIZATION NAME(S) AND ADDRESS(ES)

Naval Postgraduate School
Monterey, CA 93943-5000

8. PERFORMING ORGANIZATION REPORT NUMBER

9. SPONSORING/MONITORING AGENCY NAME(S) AND ADDRESS(ES)

10. SPONSORING/MONITORING AGENCY REPORT NUMBER

11. SUPPLEMENTARY NOTES The views expressed in this thesis are those of the author and do not reflect the official policy or position of the Department of Defense or the US Government.

12a. DISTRIBUTION/AVAILABILITY STATEMENT

Approved for public release; distribution is unlimited.

12b. DISTRIBUTION CODE

13. ABSTRACT (Maximum 200 words)

This thesis investigated the feasibility of implementing a code-division multiple-access (CDMA) local area network (LAN) employing all-optical signal processing. A two-user unidirectional data link was built and successfully tested. This data link utilized variations of optical orthogonal code sequences (OOCs) generated by serially connected fiber optic delay lines and 2x2 couplers. A special feature of this network design was use of the same hardware to decode the signal as was used to encode the signal. A detailed review of the various coding techniques and the generation of spread spectrum signals was also performed. The results of the overall system design effort demonstrated that high-data-rate signal traffic can be supported by the network and in a more power efficient and affordable manner than previous designs.

14. SUBJECT TERMS
CDMA, Fiber Optics, Spread Spectrum, Multiple Access, Delay Lines, Optical Orthogonal Code Sequences.

15. NUMBER OF PAGES
83

16. PRICE CODE

17. SECURITY CLASSIFICATION OF REPORT	18. SECURITY CLASSIFICATION OF THIS PAGE	19. SECURITY CLASSIFICATION OF ABSTRACT	20. LIMITATION OF ABSTRACT
UNCLASSIFIED	UNCLASSIFIED	UNCLASSIFIED	UL

NSN 7540-01-280-5500

i

Standard Form 298 (Rev 2-89)
Prescribed by ANSI Std 239-18

Code Division Multiple Access Local Area Network Communications
Employing Fiber Optic Signal
Processing Techniques

by

Bruce A. Legge
Lieutenant Commander, United States Navy
B.S., Illinois State University, 1978

Submitted in partial fulfillment
of the requirements for the degree of
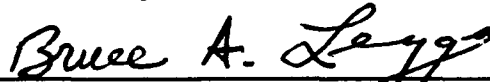
MASTER OF SCIENCE IN ELECTRICAL ENGINEERING

from the
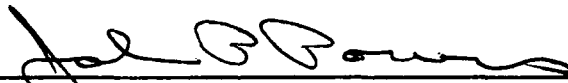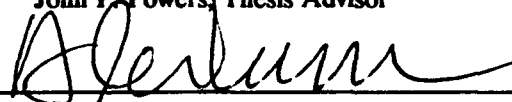
NAVAL POSTGRADUATE SCHOOL
September 1993

Author: _____
Bruce A. Legge

Approved by: _____
John P. Powers, Thesis Advisor

_____
Alex W. Lam, Second Reader

_____
Michael A. Morgan, Chairman
Department of Electrical and Computer Engineering

ABSTRACT

This thesis investigated the feasibility of implementing a code-division multiple-access (CDMA) local area network (LAN) employing all-optical signal processing. A two-user unidirectional data link was built and successfully tested. This data link utilized variations of optical orthogonal code sequences (OOCs) generated by serially connected fiber optic delay lines and 2x2 couplers. A special feature of this network design was use of the same hardware to decode the signal as was used to encode the signal. A detailed review of the various coding techniques and the generation of spread spectrum signals was also performed. The results of the overall system design effort demonstrated that high-data-rate signal traffic can be supported by the network and in a more power efficient and affordable manner than previous designs.

DTIC QUALITY INSPECTED 3

Accesion For

NTIS CRA&I	☑
DTIC TAB	☐
Unannounced	☐
Justification	

By

Distribution /

Availability Codes

| Dist | Avail and / or Special |

A-1

TABLE OF CONTENTS

LIST OF TABLES

LIST OF FIGURES

I. INTRODUCTION

A. SPECTRAL CONGESTION

Congestion of electrical signals in both commercial and military communications channels is an increasing problem. Military requirements to provide timely protection from undo interference (intentional or otherwise), along with advances in technology, forces the need for faster, less expensive, and more reliable communications. Further, prevention of signal interception may be a substantial concern. As a result, a severe strain has been placed upon the remaining spectral bandwidth. A communication technique called *spread spectrum* has been effectively utilized in several applications in order to overcome these difficulties. One of the requirements for a system to be classified as a spread spectrum system is that the transmitted signal energy must occupy a bandwidth which is larger than the information bit rate (usually much larger) [Ref. 1: p. 328]. We will later see how this technique is accomplished.

For bandwidth concerns alone, industry and the military are investing in the future by installing optical fiber as the network medium of choice instead of metal cable.

1

B. OPTICAL FIBER

Use of optical fiber as the medium in telecommunication systems offers several potential advantages over conventional communications methods [Ref. 2: p. 5]:

1. wide bandwidth,

2. light weight,

3. immunity to electromagnetic interference (EMI),

4. elimination of crosstalk,

5. elimination of sparking,

6. compatibility with modern solid-state devices, and

7. lower costs than copper-based media.

A primary objective of this thesis was to take advantage of the wide bandwidth offered by optical fibers as well as to exploit the positive attributes of spread spectrum communications.

C. SPREAD SPECTRUM COMMUNICATIONS

Several advantages accrue when using the technique of spread spectrum communications. These include resistance to jamming (anti-jamming), resistance to interference (anti-interference), low probability of intercept, and multiple user random access communications with selective addressing capability [Ref. 3: p. 855]. These advantages have led to successful spread spectrum communications in mobile-radio systems, satellite communications systems, and military applications.

1. Spread Spectrum Signals

To be considered a spread spectrum system, two criteria must be satisfied [Ref. 4: p. 404].

1. The bandwidth of the transmitted signal, $s(t)$, needs to be much greater than that of the original message signal, $m(t)$.

2. The relatively wide bandwidth of $s(t)$ must be caused by an independent modulating waveform, $c(t)$, called the spreading waveform or signal, which must be known by the receiving station in order for accurate detection to occur.

Spread spectrum signals are classified by the method in which $c(t)$ accomplishes its function. The more common techniques include *direct sequence* (DS), *frequency hopping* (FH), *time hopping* (TH), and various hybrid combinations of the same [Ref. 3: p. 855]. A brief discussion of direct sequence and frequency hopping will enhance future understanding as spread spectrum techniques are developed in greater detail.

a. Direct Sequence

Direct sequence spread spectrum is the most widely used and well known of the various spread spectrum techniques. Direct sequence spread spectrum achieves a spreading of the frequency spectrum (bandwidth) by modulating the message signal a second time using a very wideband signal (relative to the data bandwidth). This signal, $c(t)$, was defined earlier as the *spreading waveform* or *spreading signal*. The spreading signal is chosen to have properties which facilitate demodulation of the transmitted signal by the intended receiver. Equally important,

3

the spreading signal must have characteristics which makes demodulation by an unintended receiver difficult, if not impossible. These same desirable properties will also make it possible for an intended receiver to discriminate between an actual communications signal (message) and false information being transmitted by a jammer. As long as the bandwidth of the spreading signal is large relative to the data bandwidth, the spread spectrum transmission bandwidth will be dominated by the spreading signal and will be nearly independent of the data signal.

The most common and simplest form of direct sequence spread spectrum implements *binary phase-shift keying* (BPSK) as the spreading modulation. A BPSK signal has two possible amplitudes, $+1$ and -1. If the signal's amplitude is periodically switched between these values in a pseudorandom manner, a BPSK direct sequence (BPSK-DS) spread spectrum signal results. At each equally spaced time interval, a decision is made as to whether the wideband modulating signal should be a $+1$ or -1. A truly random signal sequence could be generated by tossing a coin to make such a decision. However, the receiver would not know the sequence *a priori* and could not resolve the transmitted information. Instead, an electronically generated pseudorandom sequence (approximately random) is utilized which is known *a priori* to the transmitter and receiver. Figure 1 illustrates a simplified BPSK-DS spread spectrum system. Demodulation of the spread signal is accomplished in part by remodulation with the spreading code which has been appropriately delayed. This remodulation or correlation of the received signal with the delayed spreading

waveform is called *despreading* and is a critical function in all spread spectrum systems.
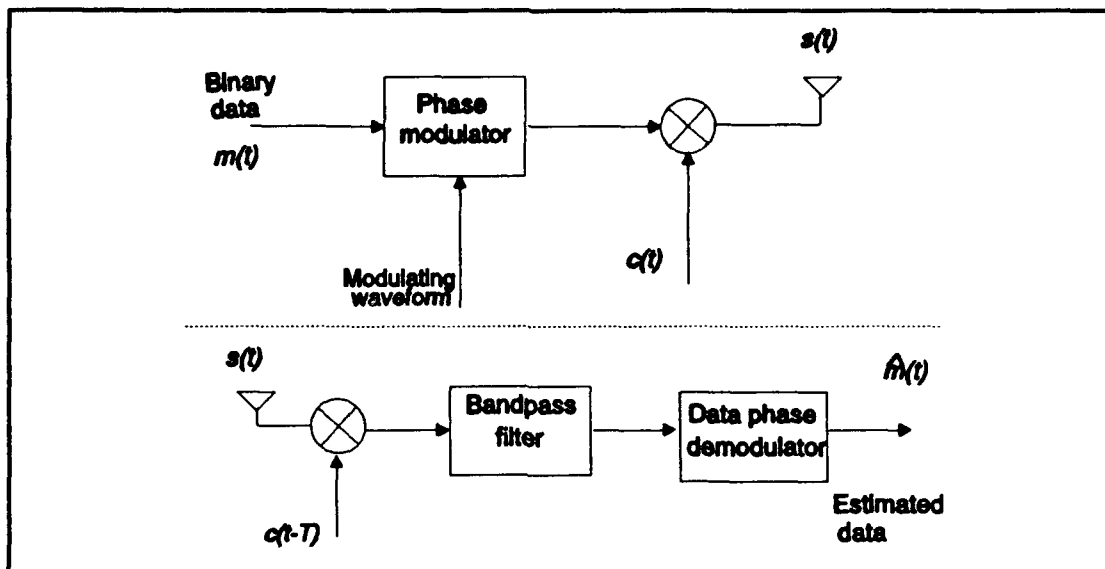
Figure 1. BPSK-DS spread spectrum transmitter (top) and receiver (bottom). [After Ref. 1: p. 333]

As previously mentioned, one of the advantages of using spread spectrum is the ability to evade jamming or, in other words, to reject deliberate interference. Interference rejection is accomplished by the receiver despreading mixer, which spreads the spectrum of the interference at the same time that the desired signal is despread. If the interference energy is spread over a bandwidth much larger than the data bandwidth, most of the interference energy will be rejected by the bandpass filter [Ref. 1: p. 337].

b. Frequency Hopping

Frequency hopping spread spectrum periodically changes the carrier frequency of the transmitted signal. This changing of carrier frequency is called "*hopping*". For example, if the allocated bandwidth is 1000 times wider than the bandwidth of the transmitted signal, then for any given time interval the signal can be transmitted at any one of 1000 possible frequencies. The result is reduced interference to any existing user [Ref. 5: p. 69].

Frequency hopping systems are basically a form of *frequency shift keying* (FSK). The difference lies in the number of possible frequencies to shift to. Simple or binary FSK (BFSK) uses two frequencies to signify a mark or a space whereas frequency hoppers may have thousands of available frequencies. Figure 2 illustrates that through the use of a frequency hop synthesizer, controlled by a pseudorandom (PN) sequence generator, the modulated carrier is sequentially hopped from one frequency slot to another into which the channel bandwidth has been partitioned [Ref. 6: p. 568].

c. Multiple Access Signals

Code-division multiple-access (CDMA) is a FH or DS spread spectrum system in which a number (two or more) of spread spectrum signals are utilized simultaneously and effectively to communicate over the same frequency band. In a CDMA system, each user is given a distinct sequence. If properly designed, these digitally coded sequences will make it possible for many users to access the channel concurrently. It should be noted that CDMA is interference

6
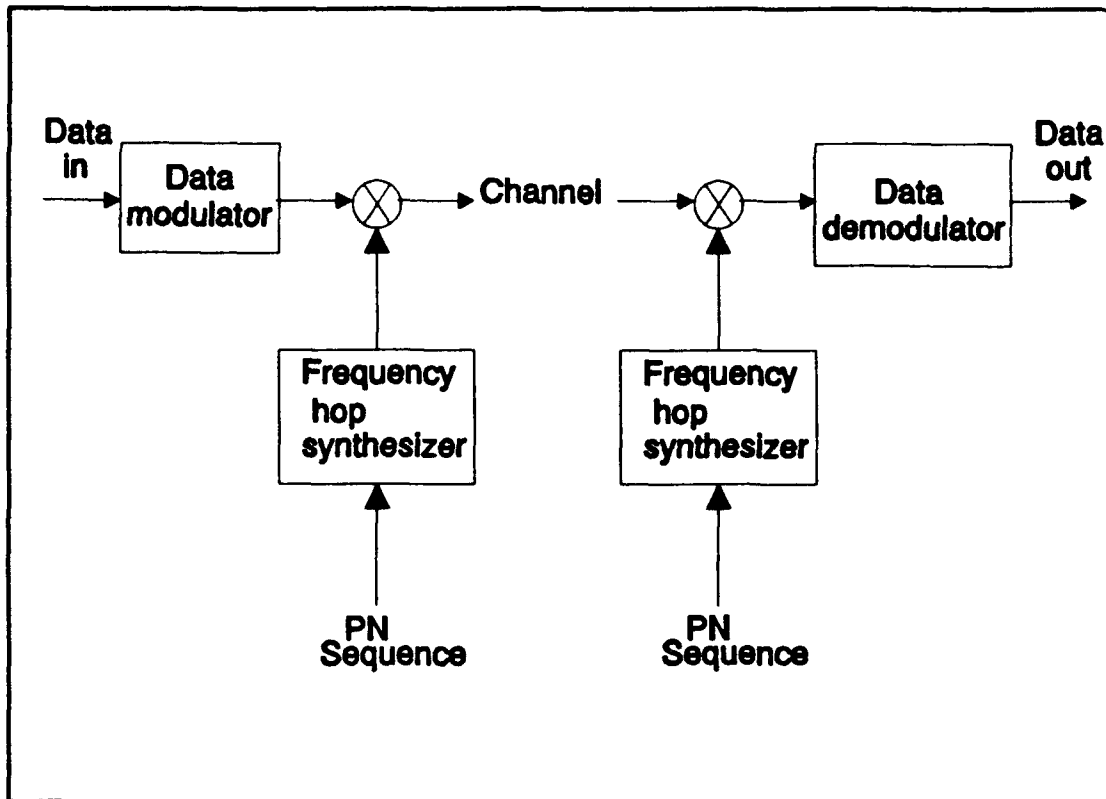
Figure 2. Frequency-hop spread-spectrum modulator and demodulator [After Ref. 6: p. 568].

limited; that is, the number of users that can use the same frequency spectrum while maintaining adequate performance is determined by the total interference power that all of the users, compositely taken, generate in the receiver of interest [Ref. 5: p. 71].

The two most commonly used multiple access schemes are *frequency-division multiple-access* (FDMA) and *time-division multiple-access* (TDMA). In FDMA, each user is assigned an equal fraction of the overall bandwidth. If an appropriately sized guard band separates each user, interference between adjacent carriers is avoided. The ability to avoid interference in FDMA results in poor utilization of overall channel bandwidth. In TDMA, the overall bandwidth is shared

7

by all users but on a time division basis. This obviously leads to very effective use of channel bandwidth. However, in links of low traffic, TDMA's expensive equipment makes FDMA the communication technique of choice.

Besides FDMA and TDMA, other systems may also employ what is known as *random multiple access* schemes to serve large populations of users with bursty (low duty cycle) traffic. This method allows users to transmit communications packets "randomly" (i.e., at will). If a collision occurs (simultaneously transmitting users resulting in data destruction), each user has to randomly select a retransmission time to avoid repeated collisions. An example of this type of random access scheme is the *Aloha* protocol developed at the University of Hawaii for interconnecting terminals and computers via radio and satellites. The major drawback of this protocol is inefficient channel utilization. Channel inefficiencies can be improved by coordinating transmissions between stations by synchronizing the transmit and retransmit timing as in TDMA. This modified *Aloha* scheme is called *slotted Aloha*. [Ref. 6: pp. 24-25, 362, 366-367]

2. Optical Signal Processing

As mentioned earlier, congestion of electrical signals throughout conventional communications channels has left little bandwidth available to employ spread spectrum techniques in certain applications. The wide bandwidth available in fiber optic networks makes spread spectrum communications an ideal choice. Until recently, the wide bandwidth available in fiber networks could not be taken fully advantage of since signal processing was required to be done electrically vice

optically. Even though fiber has been commercially available for years, optical devices capable of broadband signal processing have not. It therefore becomes desirable for an optical communications system to perform signal processing optically to exploit the tremendous potential fiber has as a transmission channel. [Ref. 7: p. 1601]

Code division multiple access schemes utilizing fibers and couplers to split, delay, and recombine short optical pulses in order to encode and decode messages have been successfully demonstrated at the Naval Postgraduate School [Ref. 8]. The use of fiber-optic delay lines alone to accomplish signal processing has a major drawback of being very inefficient in utilization of optical power due to signal splitting. This results in having to use very expensive, high-power optical sources, optical amplifiers, or being constrained to a very small local area network.

D.   THESIS OBJECTIVE

The objective of this thesis was to design a local area network (LAN) which employed code-division multiple-access techniques. The LAN utilized fiber-optic delay lines strategically connected to 2x2 couplers in a cascaded form to generate a series of pulses (i.e., to encode the data) and to subsequently decode and resolve the input "message." This technique has been previously researched and is referred to as a "ladder network" [Ref. 9]. It was shown that when two users simultaneously accessed the network that acceptable network performance was maintained despite mutual interference. Figure 3 illustrates the basic overall system design. When a

digital optical signal is fed at input 1 of user #1, a series of pulses is generated at user #1's output by the coupled multimode delay lines. This "encoded" signal is input to an *nxn* star network making the signal available to all network users. However, due to the encoding process, only the intended receiver(s) will be able to detect the message. For reception at user #1, one of the star-network outputs is fed into input 2 in order to obtain the correlation at output 3, and hence the original message is detected.

The goal of this effort was to demonstrate that a LAN utilizing a ladder network could be designed that ultimately would result in:

1. adequate performance during simultaneous access by multiple users, and

2. efficient use of optical power with economical use of resources.
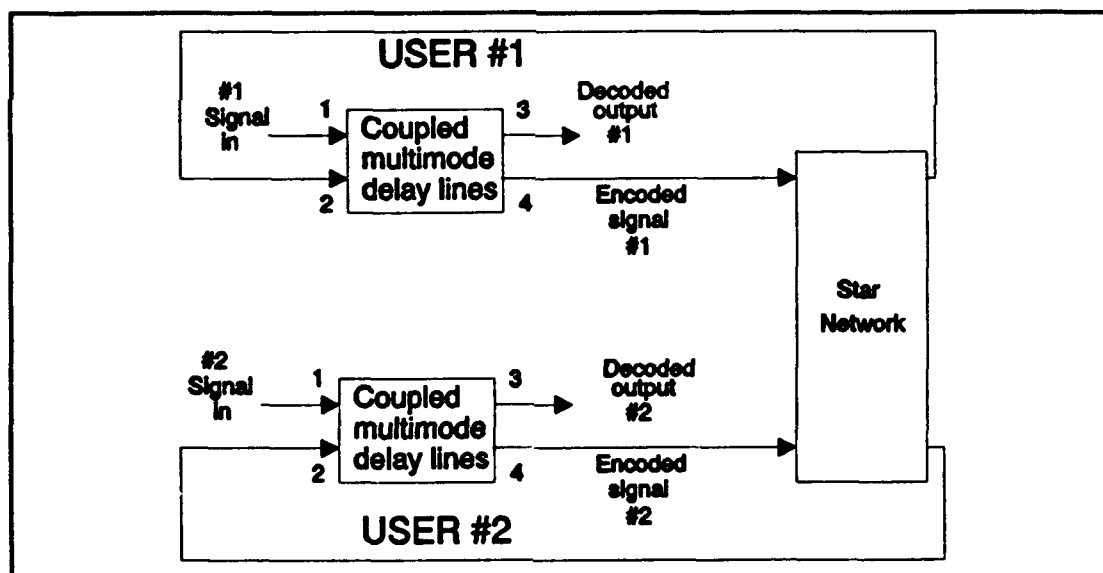
Figure 3. Block diagram of a two-user CDMA ladder network [After Ref. 9].

II. CDMA CODING TECHNIQUES

Chapter II introduces various CDMA coding techniques. After a basic overview of CDMA, properties of pseudorandom sequences will be investigated. First, electronically generated CDMA sequences (conventional sequences) will be discussed in detail. It will be shown that conventional sequences are either not compatible with fiber-optic networks or that network bandwidth would be under-utilized if they were used. Secondly, the generation and employment of *Optical Orthogonal Code Sequences* (OOCs) will be examined. It will be shown that these optically generated codes are indeed compatible with our network design and that we can take advantage of the wide bandwidth available to us in fiber-optics.

A. CDMA

CDMA is a technique used in spread spectrum communications which allows several users simultaneous access to the same frequency band. When a communications network is used for multiple access, the key to successful communications is found in the properties of the spreading waveform, $c(t)$. Spreading waveforms that have good cross-correlation properties and that have long periods will result in the best possible performance. To ensure that the spreading waveforms have desirable properties, spreading codes must be found that result in orthogonal or nearly-orthogonal properties between the different signals. A specific spreading code

will be referred to as a *codeword*. Ideally, a codeword would be infinitely long with equally likely random binary digits. This, of course, is impossible since infinite storage is not available. Thus, each codeword is chosen to be sufficiently long to ensure good cross-correlation properties between the different signals. Additionally, the number of different codewords must also be sufficiently large to ensure the network can accommodate the number of users that the network was designed to support.

The spreading waveform, *c(t)*, is usually generated by a codeword created through use of a shift register. The shift register's contents (and, hence, its output) during any time interval T is some linear or nonlinear combination of the contents of the register during the immediately preceding time interval [Ref. 1: p. 365]. Codewords used to generate *c(t)* are periodic sequences of "ones" and "zeros" with a period N. A convenient way to represent a codeword that consists of a sequence of binary digits (..., b_{-2}, b_{-1}, b_0, b_1, b_2,...) is by a polynomial having the form $b(D) = \cdots + b_{-2}D^{-2} + b_{-1}D^{-1} + b_0 + b_1 D + b_2 D^2 + \cdots$. The delay operator D implies merely that the binary symbol, b_j, which multiplies D^j, occurs during the jth time interval of the overall sequence. As a result of the codeword being a periodic sequence with period N, $b_n = b_{n+N}$ for all n. The spreading waveform or spreading signal, *c(t)*, is also periodic with a period $T = NT_c$ and is specified by

$$c(t) = \sum_{n=-\infty}^{\infty} a_n \times p(t - nT_c), \qquad (1)$$

12

where $a_n = (-1)^{b_n}$ (for BPSK), and $p(t)$ is a unit pulse beginning at 0 and ending at T_c.

The waveform $c(t)$ is deterministic, so its autocorrelation function is defined by [Ref. 1: p. 366]

$$R_c(\tau) = \frac{1}{T} \int_0^T c(t)c(t+\tau)\,dt. \qquad (2)$$

Since $c(t)$ is periodic with period T, it follows that its autocorrelation function, $R_c(\tau)$, is also periodic with period T [Ref. 1: p. 366]. Consider two unique spreading waveforms $c_1(t)$ and $c_2(t)$. The cross-correlation function of these two deterministic spreading waveforms is

$$R_{c_1 c_2}(t) = \frac{1}{T} \int_0^T c_1(t)c_2(t+\tau)\,dt \qquad (3)$$

where it is assumed that both waveforms have the same period T. The cross-correlation function is periodic as well, also with period T. [After Ref. 1: pp. 366-367]. The properties of the cross-correlation function are very important in determining the overall link performance. Specifically, it is desired that the magnitude of the cross-correlation function be as close to zero as practicable. A cross-correlation function, for example $R_{c_1 c_2}(\tau)$, that is zero-valued implies that $c_1(t)$ and $c_2(t)$ are orthogonal waveforms. This would be the ideal situation; however, in the majority of applications utilizing multiple access spread spectrum communications, nearly orthogonal conditions must be accepted. Bit-error rate

13

performance deteriorates as the magnitude of the cross-correlation function increases, which occurs as the spreading waveforms become increasingly correlated.

The selection of a set of spreading waveforms to be used within a multiple access network are carefully chosen to have desirable properties such that the spread spectrum system operates at maximum efficiency. For example, the phase of the received spreading code, $c(t-T)$, must be originally determined (acquisition) and then tracked (maintaining synchronization) by the receiver. This is accomplished by various phase-locked loop designs. To facilitate these functions, $c(t)$ is chosen to have a two-valued autocorrelation function. As mentioned before, good cross-correlation properties are a must in multiple access applications. When potential jamming is a concern, spreading waveforms are selected that have extremely long periods which are nearly impossible for the jammer to predict and duplicate. [Ref. 1: p. 365]

Once a message has been coded and spread, it is sent over a channel where noise and possibly interference modify the original message. A receiver demodulates and recovers the original message by despreading and filtering the received signal. Figures 1 and 2 (on pages 5 and 7, respectively) illustrate basic block diagrams of spread spectrum receivers which despread the received signal by a correlation process. Further, based on the amount of energy in the despread and filtered signal, an evaluative decision is made as to as to the accuracy of the received signal's phase and frequency. Figure 4 gives a basic block diagram of a typical system used to evaluate a single spreading waveform phase and frequency. It should be noted that

the spreading waveform generator produces an exact replica of the spreading code sequence unique to that particular data signal.
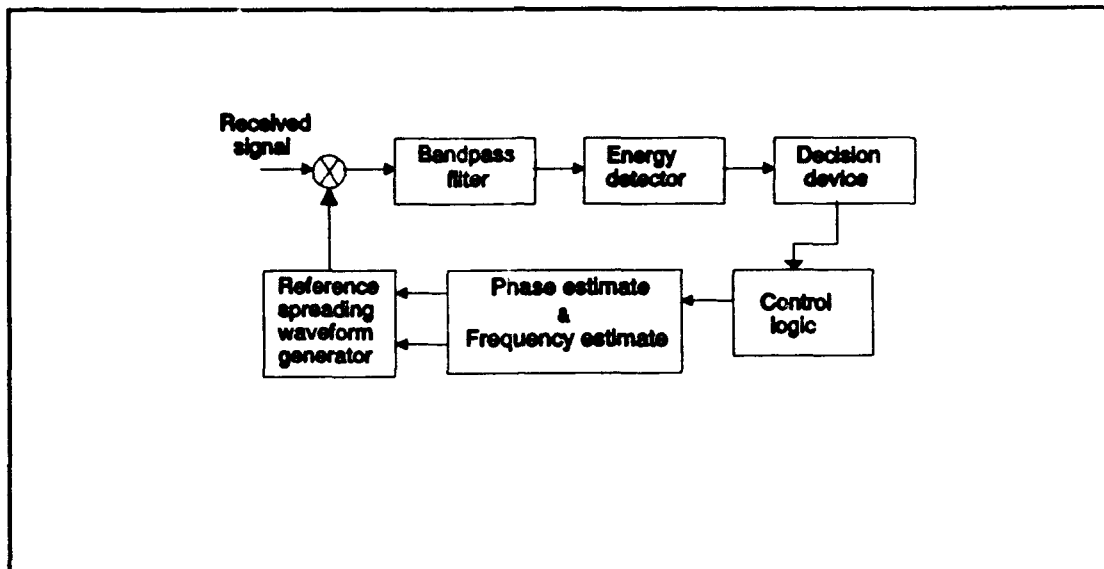
Figure 4. System used to evaluate a single spreading waveform phase and frequency. [Ref. 1: p. 487]

B.   SEQUENCES FOR SPREAD SPECTRUM SYSTEMS

1.   PN Sequences

Both frequency hopping and direct sequence spread spectrum communications use pseudorandom sequences to generate the necessary spreading properties as the "fair coin toss experiment." These properties include the following (assuming that binary phase shift keying is used as the spreading modulation) [Ref. 5]:

1.   In a sufficiently long sequence, about 50% of the chips will be $+1$ and 50% will be -1.

2. The autocorrelation of the PN sequence will be very small except in the vicinity of $r = 0$.

3. The cross correlation between any two different PN sequences will be small.

The length of the code sequences in conventional CDMA applications are of much greater length than those utilized in the usual areas of coding for transfer of information since they are intended for bandwidth spreading and not for direct transfer of information. We shall see that, when using OOCs, the shorter sequences are more desirable (assuming that the required number of users can be supported) since they allow a higher data rate to be used. The importance of the type of code, the length of code, and the chip rate cannot be overemphasized, as these characteristics set the bounds for the systems overall performance. The capability of the system can only be changed by changing the code.

The properties of codes used in spread spectrum systems in which we are most interested are summarized as follows [Ref. 10: pp. 56-57]:

1. *Interference protection.* Coding allows a trade-off between overall system bandwidth and processing gain. Processing gain, N, is defined as the ratio of the spread to unspread bandwidth [Ref. 4: p. 410].

2. *Provision for privacy.* Coding enables protection from eavesdropping to the extent in which the codes themselves are secure.

3. *Noise-effect reduction.* Error-detection and error-correction codes can significantly reduce the undesirable effects of noise and interference.

16

2. Conventional CDMA Sequences

Each bit in a CDMA system is encoded into a waveform, $s(t)$, which corresponds to a code sequence of N-chips. These N-chips represents the destination address of that bit. Each receiver performs the correlation between its own address, $f(t)$, with the received signal $s(t)$. The receiver output, $r(t)$, is

$$r(t) = \int_{-\infty}^{+\infty} s(z) f(z-t) dz. \tag{4}$$

If a signal arrives at the correct destination, then $s(t) = f(t)$ and (4) represents an autocorrelation function. If a signal arrives at any destination other than its own, (4) represents a cross-correlation function since $s(t) \neq f(t)$. In order for each receiver to maximize the discrimination between the correct signal and all other signals (interference), it is necessary to maximize the autocorrelation function and minimize the cross-correlation function. This is accomplished by selecting code sets which are orthogonal or nearly orthogonal. [Ref. 11]

a. Maximal-Sequences

Maximal codes are the longest codes that can be generated by a shift register or a delay element of a given length. In binary shift register sequence generators, the maximum length sequence consists of $2^n - 1$ chips, where n is the number of stages in the shift register. A shift register sequence generator consists of a shift register and logic gates which feed back various logical combinations of the state of two or more stages back to the input of the register. The output of a

17

sequence generator and the contents of its stages at any given time are a function of the current and previous state of each individual stage [Ref. 10: pp. 58-59]. Figure 5 illustrates the general layout of a simple linear generator (three-stage maximal generator). Outputs from the last delay stage D_3 and intermediate stage D_2 are combined in a modulo-2 adder (an EXCLUSIVE OR (XOR) gate in simplest form) and fed back to the input of the first delay element. Table 1 displays the order in which the delay elements take on seven different states, (there are 2^n-1 possible states with $n = 3$), assuming that state 1 is the starting condition. Observe the random appearance of the output as would be seen by a viewer not knowing the length or order of the sequence. A very important characteristic of maximal length codes is that their autocorrelation function is two-valued and is given by [Ref. 11]:

$$r(t) = \begin{vmatrix} N, & t=0 \\ -1, & t=i\dfrac{T}{N} \end{vmatrix} \tag{5}$$

where T is the bit duration, N is the length of the sequence, and i is an integer with values of ± 1, ± 2, $\cdots$. This characteristic makes a maximal length sequence easy to distinguish from time shifted versions of itself. The function described by equation can be viewed graphically in Figure 6 where the autocorrelation function has been graphed as a function of τ.

modulo-2 adder (XOR gate)

D₁ D₂ D₃ Code output

Three-stage maximal generator (simple type)
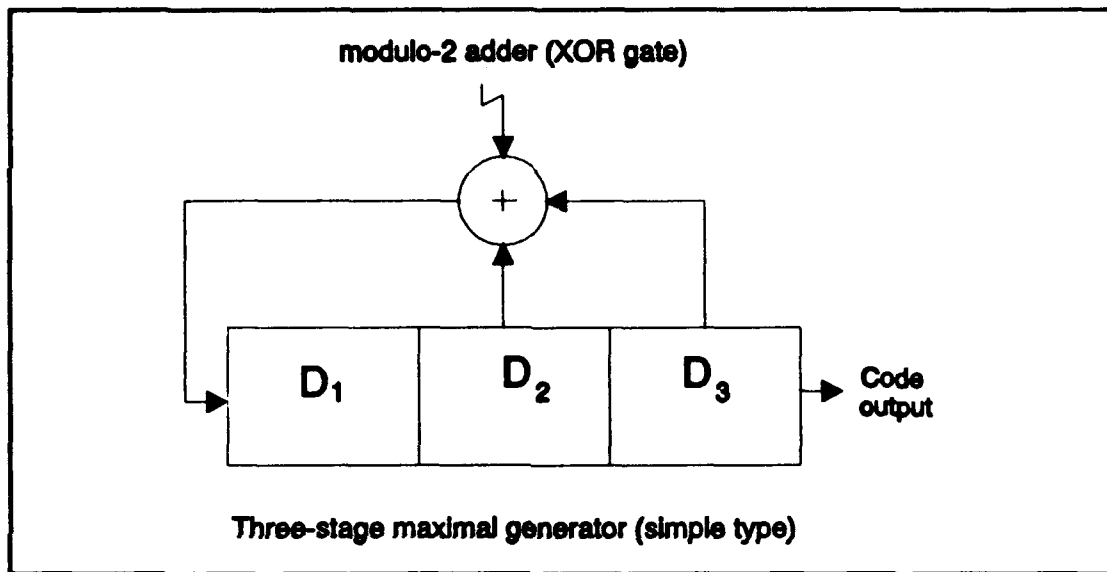
Figure 5. Typical code sequence generator (simple type). [After Ref. 10: p. 65]

Table 1. BINARY-TO-DECIMAL CONVERSION OF THE OUTPUT OF A THREE STAGE REGISTER DEMONSTRATING PSEUDORANDOM ORDERING.

Output of delay element				
State	D_3	D_2	D_1	Base-10 value
1	1	1	1	7
2	1	1	0	6
3	1	0	0	4
4	0	0	1	1
5	0	1	0	2
6	1	0	1	5
7	0	1	1	3

19

A major problem associated with some maximal length sequences is that the lower bound for the peak of the cross-correlation function is no less than $-1+2^{(n+1)/2}$. This suggests that certain maximal length sequences will interfere strongly with one another. The code sequences that exhibit the minimal cross-correlation peak ($-1+2^{(n+1)/2}$) are usually referred to as *preferred maximal length sequences*. Since the set of preferred maximal length sequences is small, the use of maximal length codes is not compatible with CDMA spread spectrum communications, where a large number of unique addresses is required. [Ref. 11]

b. Gold Codes

Special codes called *Gold codes* are attractive for use in CDMA in that there are a large number of orthogonal sequences available. This translates directly into an increase in the number of users a channel can support for a given bit error rate. Gold codes are generated by combining a pair of preferred maximal length sequences through modulo-2 addition [Ref. 11]. A desirable result of generating a Gold code is that the cross-correlation function is bounded. The maximum value that the peak of the cross-correlation function can attain is equal to that of the generating maximal length sequence pair [Ref. 11].

The performance of a network utilizing Gold codes is a function of the number of simultaneous users, K, and the length of the coded sequence, N. The channel's signal-to-noise ratio (SNR) is represented as the square of the autocorrelation function's peak to the variance of the amplitude of the interference.

20

It is assumed that all interference (noise) results from other users and perfect synchronization is maintained between transmitter and receiver [Ref. 11]. The *SNR* for Gold codes has been shown to be [Ref: 12]:
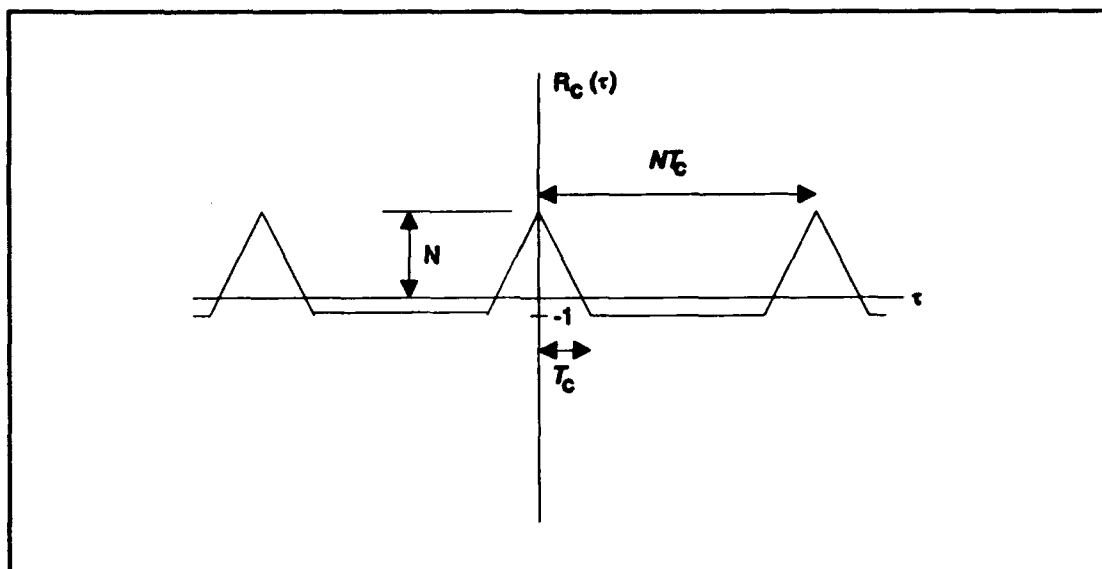
Figure 6. Autocorrelation function for a maximal-length sequence with chip duration T_c and period NT_c [Ref. 1: p. 388].

$$SNR_{conventional} = 4 \left[\frac{N^3}{(K-1)(N^2+N-1)} \right] \qquad (6)$$

The variance of the cross-correlation function (SNR denominator) is easily seen to increase as the number of simultaneous users and/or number of chips increases. Unfortunately this translates directly into a decrease in SNR and an increase in probability of bit error. The (K-1) term in the expression for the SNR is a result of assuming K-users are simultaneously transmitting and that all interfering signals are uncorrelated. Thus the variance of the total interference is equal to the

21

sum of K-1 identical cross-correlation functions [Ref. 11]. Figure 7 illustrates how the SNR for Gold codes varies as a function of the number of users (N is fixed). It is clear from Figure 7 that for a given number of chips per bit, the *SNR* gradually decreases as the number of users increases. This translates directly into an increase in probability of bit error. Hence, more users accessing the network at any given time implies poorer system performance.
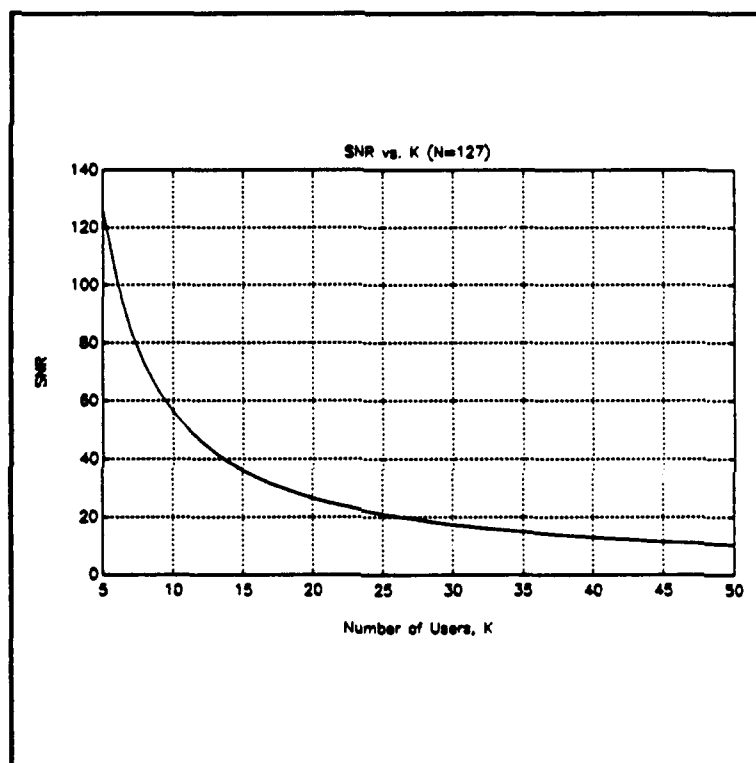
Figure 7. SNR versus number of simultaneous users (N = 127).

An optical conventional CDMA system using Gold codes was reported in Reference [12]. Transmission of the signals were over optical channels; however, the signal processing was performed electronically. The speed of this system design

22

was limited by the processing speed of the electronics, thus failing to take full advantage of the available resources offered by fiber optics.

The CDMA system which is presented next uses all-optical processing. The new CDMA sequences designed specifically for use in optical processing systems are called *Optical Orthogonal Code Sequences* (OOCs). The new all-optical CDMA system has the potential for an increase in the number of chips per bit (wide bandwidth system), hence an increased capacity over systems using electronic processing.

3. Optical Orthogonal Code Sequences

A fundamental difference exists between optical processing and conventional processing. To illustrate this difference, the use of tapped delay lines presented in Reference [13] will be examined. Conventional delay lines combine tapped signals coherently. On the other hand, in most instances optical fiber delay lines combine tapped signals incoherently. This incoherent signal combining results simply in summation of optical power. Figure 8 can be used to illustrate the difference between coherent and incoherent combining of signals [Ref. 11]. The weights a_j equal the code sequence that corresponds to the appropriate destination address. The values of the a_j equal $+1$ or -1 for conventional processing, and $+1$ or 0 for incoherent optical processing. When the received coded data matches the values of the weights a_j after being appropriately delayed, the correlator output will be at a maximum (autocorrelation). The value of the correlator output will be less than the autocorrelation peak any time the received coded data is for another

23

address, or, if the address is correct, has not yet been matched to the weights a_j. Conventional communication systems are often based on $+1/-1$ signals which take advantage of the ability to add the signals to zero in order to achieve true orthogonality. Reference [14] investigates whether coherent optical CDMA (a better parallel to radio-frequency (RF) techniques) could be implemented with beneficial results.
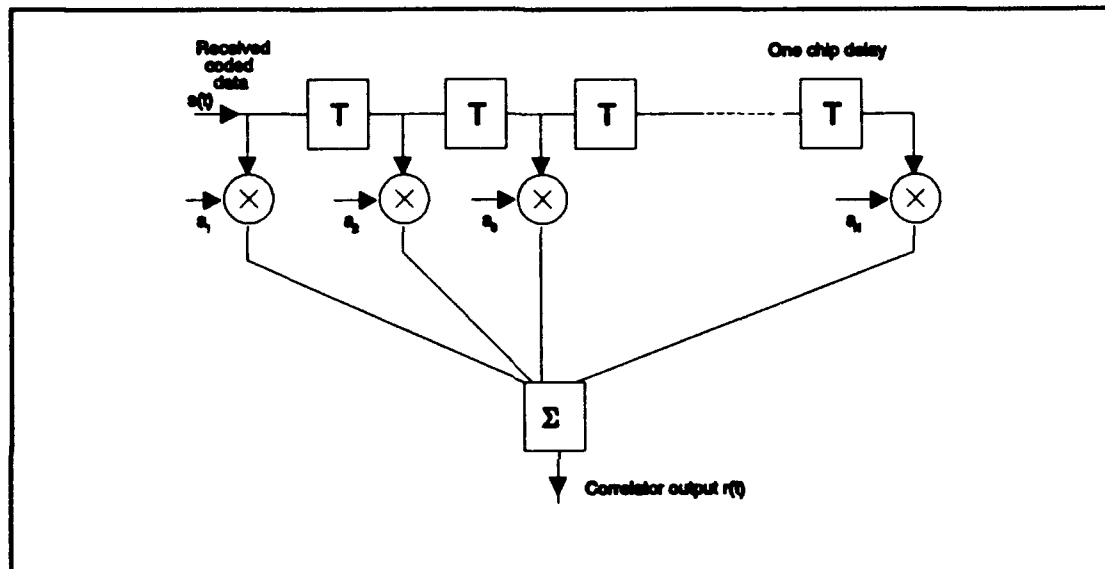
Figure 8. Block diagram of the correlation process for conventional or optical signal processing.

Employing incoherent optical processing, the levels $+1$ or 0 of the transmitted optical code sequence correspond to light "ON" or light "OFF". The weights a_j in Figure 8 are set to 0 at positions corresponding to light "OFF" in the correct code sequence and set to $+1$ at positions corresponding to light "ON" in the correct code sequence. Therefore, the peak of the autocorrelation function for this correlator is equal to the total number of 1's in the code sequence. The peak of any

24

cross-correlation function (assuming multiple users) equals the maximum number of coincident 1's in all shifted versions of the different code sequences. In contrast, the number of 1's in each Gold code sequence varies and, therefore, so does the peak of the autocorrelation function. Additionally, the number of coincident 1's between shifted versions of two code sequences can be large and, therefore, so can the peak of the cross-correlation function. Gold codes are consequently unacceptable for this type of incoherent optical signal processing. For this reason, a new set of codes is needed which has fewer coincident 1's between all shifted versions of the various code sequences. [Ref. 11]

Orthogonality requires that the value of the cross-correlation function be equal to zero. In incoherent optical signal processing, it is not possible to achieve strict orthogonality. As mentioned before, incoherent signal combining results in power summation. Thus, fiber optic signal processors are modeled as "positive systems". A positive system is one that cannot manipulate its signals such that it adds up to zero. Incoherent fiber optic signal processing, however, is equivalent to power measurement, and, since power is a non-negative quantity, such signals cannot be optically manipulated such that the summation adds to zero. [Ref. 15]

The new set of code sequences that we desire are called *Optical Orthogonal Codes* (OOCs). OOCs are zero (off) – one (on) sequences, which we will note as (0,1), which have a maximum value for their cross-correlation function equal to one. OOCs can be considered pulse waveforms in which a 1 corresponds to the location of an optical pulse, while zero corresponds to the absence of a pulse. For

25

reasons of power conservation, an OOC has many more 0's than 1's in each codeword. In contrast, a $+1/-1$ sequence is designed to have equal numbers of $+1$'s and -1's. It will become apparent why this is and must be the case. [Ref. 16]

An amicable feature of OOCs is that they can be calculated off-line and then applied to the CDMA system when needed. This simplifies the network implementation as well as reduces the number of required components. Additionally, by using incoherent detection, no synchronization is required between the transmitter and receiver. Signal detection is accomplished by using a matched filter (correlation process), followed by a threshold detector, and finally a pulse generator which triggers each time it is concluded that a "1" was received. [Ref, 8: p. 18]

Reference [16] presents a detailed study on the theory and generation of OOCs. Sequences with weight up to five (i.e., the number of 1's is five) were studied which would support a network of up to fifteen users. The results of this study were displayed in a useful, tabular form.

A code set is represented as the function $g(r,n)$ where r is the number of users (each with a unique code), and n (code weight) is the number of "1's" in the sequence. Sequences will be represented as vectors. For example, denote $\underline{X} = (x_1, x_2, \cdots x_L)$ and $\underline{Y} = (y_1, y_2, \cdots y_L)$ where $\underline{X}$ and $\underline{Y}$ are two distinct sequences, each with length $= L$. $\underline{X}$ and $\underline{Y}$ are said to form a pseudo-orthogonal (0,1) code set if the autocorrelation functions and the cross-correlation function satisfies the following:

Autocorrelation function,

$$C_{xx}(t) = \begin{bmatrix} n & t=0 \\ \leq 1 & t \neq 0 \end{bmatrix} \qquad (7)$$

Cross-correlation function,

$$C_{xy}(t) \leq 1 \; for \; all \; t. \qquad (8)$$

Table 2 presents the actual codes utilized in this thesis. These codes represent a weight four, two-user sequence set of lengths ≥ 14 and ≥ 12, respectively. Zero padding of the sequences has absolutely no effects on the sequence properties, hence the length of both sequences can be fourteen. The numeric values within the table represent the location of the pulse relative to the 14 possible locations. For example. a "4" represents a sequence of (0,0,0,1,0,0,0,0,0,0,0,0,0,0).

Table 2. SEQUENCE SOLUTION SET [After Ref. 16: Fig. 3].

Pulse Location For				
user	g(2,4)			
1	1	4	13	14
2	1	6	8	12

Chapters I and II have introduced the different types of spread spectrum signals and coding techniques. Both advantages and disadvantages were discussed

27

which led to the various signaling and coding schemes that were required to be employed. Chapter III will center on the actual implementation of the system design and the factors which led to its composition.

III. SYSTEM DESIGN OBJECTIVES/OVERVIEW

A. SYSTEM LAYOUT

The basic system layout revealed in Figure 9 has been expanded to include details not found previously in Figure 3. This specific design is for a two-user network; however, in larger capacity networks other users can easily be accommodated by connecting their ladder structures directly to the *nxn* coupler (star coupler). This design is limited nevertheless to a fixed maximum number of users that can simultaneously access the network without exceeding a predetermined allowable bit-error rate. In other words, the network is interference limited. Reference [16] provides a method and a detailed discussion on the calculation of the minimum length that an OOC must have to support a fixed number of users with a fixed code weight. This length is given by:

$$L \geq \frac{NK(K-1)}{2} + 1, \tag{9}$$

where L is the sequence length, K is the code weight (number of 1's), and N is the number of OOCs in the code set. Possibly cost, equipment availability, etc., could constrain us to a fixed sequence length. This being the case, we would be interested in how many users the network could support. Rearranging Equation (9) and solving for the number of users we obtain:
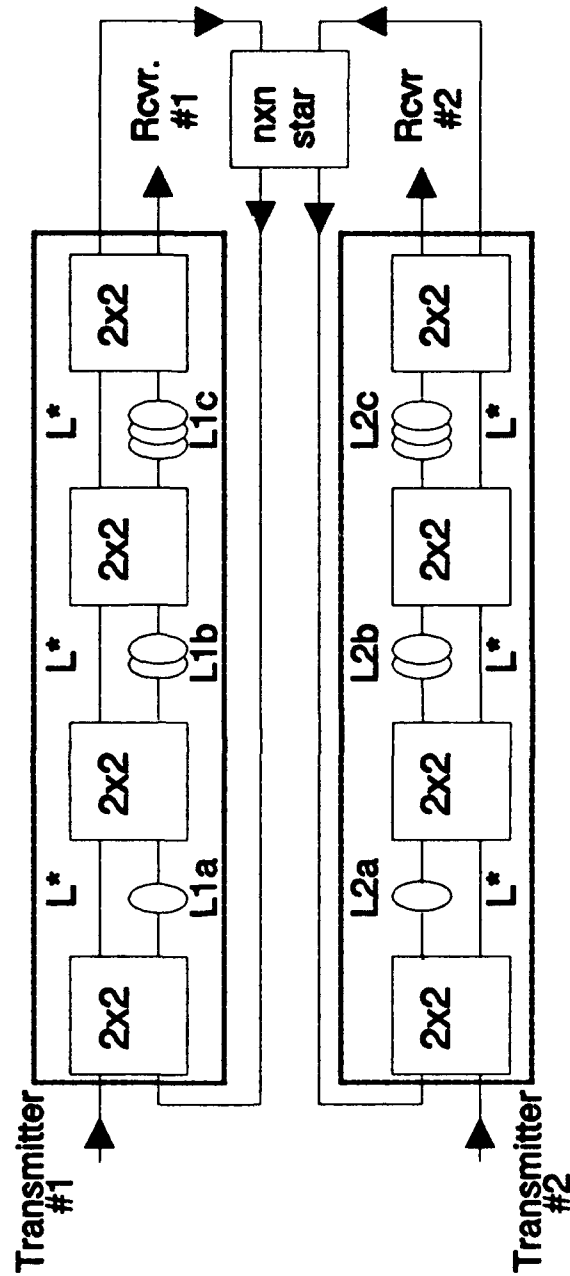
Figure 9. Two-user CDMA ladder network.

30

$$N \le \frac{2(L-1)}{K(K-1)}. \tag{10}$$

The maximum number of possible users, N, would then be rounded down to the closest integer value. This equation, however, is subject to the constraint that $2(L-1) \ge K(K-1)$. Figure 10 shows graphically how the number of possible users varies as a function of the code weight for the following fixed values of code length: $N = 16$, 32, 64, and 128.
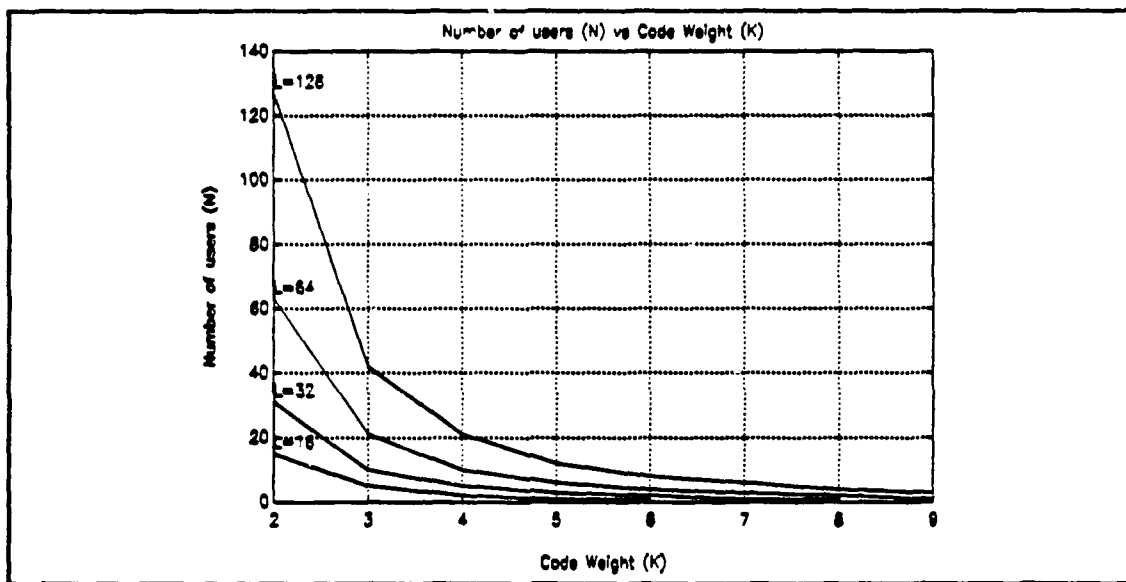
Figure 10. Maximum possible number of users vs. code weight (code length L is fixed).

One observes that, to support a reasonable number of users (say at least 10), the code weight must be 4 or less for $N = 64$ and 5 or less for $N = 128$. It must also be noted that the bit error rate increases as the ratio of the autocorrelation function peak to cross-correlation peak decreases. This occurs as the code weight is decreased while maintaining the same number of users and the same code length. As

mentioned earlier, it is desirable to keep the code-sequence length as short as possible to maintain as high a data rate as possible. One recognizes that a compromise (trade off) must be made between cost and performance in terms of supporting a given data rate at a specified bit error rate.

As we refer to Figure 9, we must remember that the network was designed to support two users using a code weight of four with a code length of fourteen. These specifications satisfy the requirements of Equations (9) and (10) and, moreover, were chosen to enhance understanding and provide for ease of discussion. Concept demonstration was accomplished in a more comprehensible fashion than would be achieved in a more extensive and complicated network.

To understand the operation of the system in Figure 9, we begin our discussion by referring to the upper-half of the drawing only (User #1). Transmitter #1 emits a narrow pulse of light into the first 2x2 coupler (or splitter). The pulse power is divided in half (theoretically) by the splitter and a pulse, with one-half the original amplitude, emerges from the splitter on each of the delay lines. Due to the differences in length between the fixed (length=L^*) delay line and the variable (length=L1a) delay line, the pulses arrive at the second splitter at different times. It should be noted that the length of the variable delay line is always greater than the length of the fixed delay line. This means that the pulse traveling on the fixed delay line will reach the following coupler first. The pulses are combined and split by the second splitter resulting in a series of two pulses (now at one-fourth the original amplitude) which emerge from each output of the second splitter. Similarly, the

32

pulses are combined and split by the third and fourth splitter in such a manner that emerging from the final splitter is a series of eight pulses on each fiber, each with an amplitude equal to one-sixteenth of the original amplitude. Four of these eight pulses make up the OOC, referred to as user #1 in Table 2 on page 27, which has a code weight equal to four. It will be shown later how the actual lengths of the variable delay lines were determined, but suffice it to say that the lengths are such that a pulse exists at each of the pulse locations required in the table (Table 2).

One set of eight pulses, which exist on each output of the final splitter (which will be referred to as the encoded signal), enter the star network (actually a 2x2 coupler in this design) and are distributed to each receiver at one-half the input amplitude. The star is a unidirectional (non-reciprocal) device, providing high cross-input rejection (inputs are isolated from one another) [Ref. 8: p. 23 and Ref. 2: p. 61].

A replica of the encoded signal (eight pulses on the other delay line) is routed back to the input of the first 2x2 coupler to be sent through the series couplers of user #1 once again and in the same order as the first time (decoder). The purpose of this second pass is to perform the cross-correlation with the message signal being received at transmitter #1. Since the received message is the same as the transmitted message in our case, the cross-correlation reduces to an autocorrelation. The autocorrelation results because the series couplers now act as a matched filter with respect to the original signal. The peak of the matched filter response occurs at the time equivalent to the time it take a pulse to travel the distance equal to

33

L1a+L2a+L3a. During this second pass, no further net splitting losses occur since each time a pulse at the location specified in the OOC exits the splitter, it is split but then added to one of the other pulses which has been properly delayed such that it overlays the OOC pulse (power summation). Insertion losses still occur, however, but they are small relative to splitting losses.

The output of the "matched filter" (output of last 2x2 splitter) is sampled at the proper sample time (the peak of the matched filter response) and would be input to some type of decision device. The decision device would be set at a pre-selected threshold necessary to achieve a certain total error probability and false-detection rate. (This decision circuitry was not added to our circuit.)

We note several important facts based on the chosen system design:

1. Coding and decoding of the signal is accomplished with the same optical hardware. This reduces the overall system costs and complexity.

2. The system allows access at will (asynchronous operation); no network access-control is required.

3. The power losses due to the splitters in this approach (serial data flow) is 6 dB less than in previous approaches (parallel data flow). This fact will be demonstrated in our discussion of power budget calculations.

4. The cross-correlation performed at the decoder of one user with the encoded message of another user will not result in message detection. This is due to the approximate orthogonality between OOCs.

B.   DESIGN CONSIDERATIONS

The starting point for designing a link begins with selection of the operating wavelength, the type of source (LED or laser), and whether a single-mode or multi-

mode fiber will be used. One either knows or estimates the required data rate needed to meet system specifications. From this data rate and an estimate of the link distance, one chooses the wavelength, type of source , and type of fiber. [Ref. 2: p. 271]

1. Bit Rate

Instead of designing the link based on an estimate of the required data rate, we begin by selecting the chip period, T_c, such that it is the shortest interval that available equipment can support. The length of the code-sequence, L, determines the number of chips in each data bit period, T_b. Hence, we can state the following relationship:

$$T_b = L \cdot T_c. \tag{11}$$

Once again we note that the chosen code length was fourteen, as seen in Table 2 on page 27. Thus, each bit of data will be divided into fourteen equal time slots. It was determined that a chip period of 10 nanoseconds could be supported by equipment available within the laboratory. From Equation (11), we easily calculate the data bit period, T_b, to be 140 nanoseconds. From the relation $R_b = 1/T_b$, where R_b is the data rate, we determine for the available laboratory equipment that $R_b = 7.14$ *Mb/s* is theoretically the highest supportable data rate.

2. Fiber Type

We have a choice between two types of fiber, single-mode fiber and multimode fiber. Single-mode fibers are superior in applications requiring long distances at high data-rates. The advantages of high data-capacity and low attenuation have overcome the shortfalls of difficult fabrication tolerances and difficult coupling of light from the source. At present, single-mode fibers are competitive in price with multimode fibers. [Ref. 2: p. 40]

Multimode fibers are often used in applications requiring only moderate distances, moderate data-rates, or both. Their core size is much larger making the coupling of light much easier. Multimode fibers are also not as susceptible to excess losses due to bends and losses due to core-diameter fluctuations (caused by handling) as single-mode fibers. The primary disadvantage, as compared to single-mode fibers, is the relative lack of bandwidth capacity. [Ref. 2: p. 40]

The use of 50/125 multimode graded-index fiber was chosen for our network design. (This notation infers a 50 μm fiber core diameter and a 125 μm fiber cladding diameter.) This fiber type was chosen due to the relative ease of attaching connectors to it as well as it being available in large quantities. Additionally, moderate data-rates and short distances were being used which multimode fiber will support very favorably.

3. Wavelength

The design of our network can support any of the common operating wavelengths. It would be desirable to operate at 1550 nm, due to this being the

wavelength corresponding to the minimum attenuation (dB/km); however, for laboratory use, the cost of 1550 nm transmitters and receivers are in general higher than those for other wavelengths. The use of 850 nm sources and receivers, along with their low cost, would be compatible with this network design; however the flexibility to increase link distances and increase data-rates would be missing due to the larger attenuation. A wavelength of 1550 nm was chosen for testing our design due to the benefits of low attenuation and for cost reduction since the source was already on hand in our laboratory.

4. Sources

Two types of sources are presently available for use in our fiber-optic network. These sources are light emitting diodes (LED) and laser diodes. Sources are classified according to wavelength. *Short-wavelength sources* produce light in the range 500-1000 nm. *Long-wavelength sources* produce light in the range 1200-1600 nm. The short-wavelength devices are lower in cost, and more available than their counterparts, but suffer greater attenuation. The long-wavelength devices are chosen specifically for applications requiring minimal fiber losses and dispersion effects. Since an operating wavelength of 1550 nm has been chosen, we want to concentrate on actual source selection. [Ref. 2: p. 105]

Table 3 summarizes the important properties of LEDs and laser diodes which must be considered prior to selecting the optimal source. One notices immediately that the laser diode holds a significant operational advantage over the LED with the exception of cost and temperature dependance. The problem of

37

temperature dependance can be overcome through the use of a variable heat sink device (also adding to the overall cost) which will keep temperature essentially constant. Thus, if one can afford the cost of a laser diode, this is the source of choice. [Ref. 2: pp. 106-168]

Table 3. PROPERTIES OF LEDS AND LASERS.

	Surface Emitting LED	Edge Emitting LED	Laser
Power Coupled into Fiber	-38 to -13 dBm	-38 to -13 dBm	> -10 dBm
Fiber Type	multimode only	single or multimode	single or multimode
Spectral Width	100 nm	60-80 nm	< 5 nm
Rise Time	10's of nanoseconds	10's of nanoseconds	10's - 100's of picoseconds
Added Noise	essentially none	essentially none	must consider
Temperature Dependance	not significant	not significant	threshold current increases exponentially with temp.
Reliability	good; lifetime = 10^5 - 10^8 hours	same as surface emitting LED	good at moderate temp.; 10^5 hours or more
Cost	1/2 laser cost	1/2 laser cost	2 X LED cost

It appears that a high quality LED would be sufficient for use in this two-user CDMA network since the problems of a parallel network (high attenuation) have been overcome. This in general would be the case except that planned growth of the network would not be possible. Thus, to achieve a proper balance between overall system cost and planned growth, laser diodes operating at 1300 nm were chosen.

A TEK TFP2 FiberMaster Optical Time Domain Reflectometer (OTDR) was chosen to be used as the test source for this network. Reference 17 is the operator manual for the OTDR. The OTDR was on hand prior to commencement of this thesis which minimized the cost of research. This specific OTDR was equipped with a 1550 nm laser source (a 1300 nm source was not available in our OTDR) which could produce pulses with pulse-widths ranging from 10 ns to 10 μs. The network was designed to accommodate the 10 ns pulse in order to achieve the highest possible data rate.

Figure 11 is the waveform produced following detection by a Photodyne 1600XP Optical Waveform Analyzer after sending a 10 ns pulse through the network. This waveform was captured with a Tektronix transient digitizer being operated in accordance with Reference 18. A hard copy of the waveform was obtained using a Hewlett Packard 7470A Plotter. For completeness, a description of the symbols and measurements which are displayed in Figure 11 is given.

Two cursors are displayed in the waveform window and are identified by "v" and an inverted "v". The letter "T" in the waveform indicates its trigger point. The

39

area above the waveform window is called the cursor readout. The measurements displayed in this area are made relative to the position of the two cursors and the trigger point. For instance, V1 is the voltage level associated with cursor 1 (inverted "v"). The value "t1" is cursor 1's time position relative to the trigger point. The values "DV" and "Dt" are the voltage and time differences between the current cursor positions. The lower section of the waveform window displays the currently displayed record number, R1, and a time stamp indicated by "0S". The time stamp indicates the trigger point time on the currently displayed record relative to the trigger point of the record #1 acquisition. Record 1 (R1) is always 0 [Ref. 18: p. 3-29]. The shaded region in the lower right-hand side of the window is called the record bar. It provides an approximate location of the current display, the trigger event, and the cursor locations relative to the entire record. The channel status is displayed to the left of the waveform window. It provides a display of the source channel, input range, offset, and vertical expansion factor. Lastly, the small ground symbol at the left axis indicates the zero-volts reference level.

Note also from Figure 11 that the laser source produces very clean, sharp waveform edges as well as a distinct 10 ns pulse as evidenced by the value indicated next to "Dt".

5. Detector

As previously mentioned, a Photodyne 1600XP Optical Waveform Analyzer was used as the detector for this network. The Model 1600XP converts optical signals into corresponding electrical output signals. A flat frequency response is obtained

40
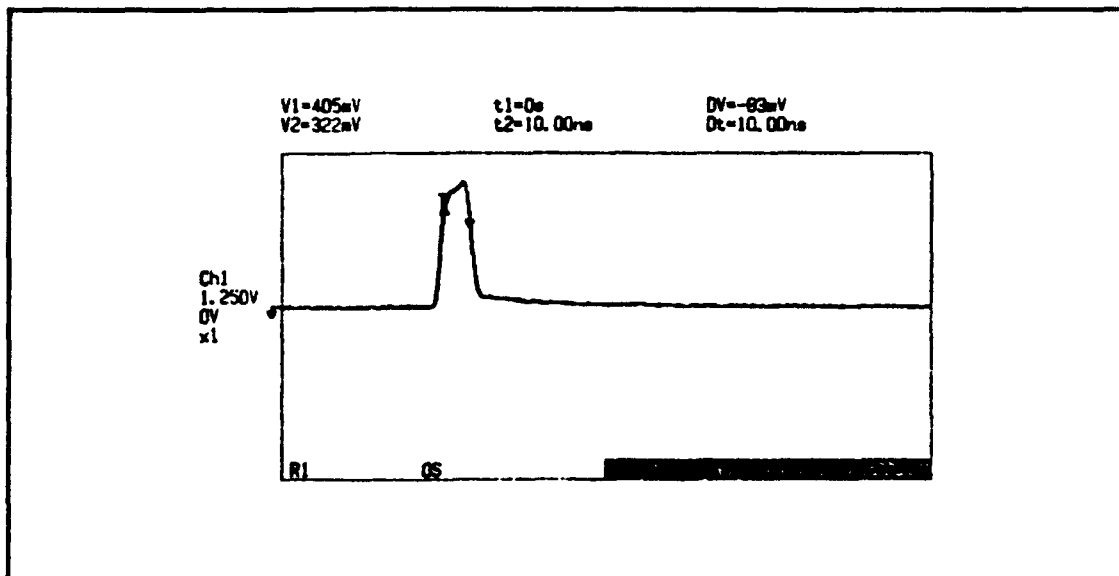
Figure 11. Waveform of OTDR laser test source.

when optical signals, in a wavelength range of 800 nm to 1600 nm, are received from DC to 150 MHz. This wide band frequency response along with the rapid rise/fall times (rise time + fall time ≤ 4 ns) makes this detector a satisfactory choice for our network application. The Model 1600XP also provides three choices for the expected range of optical power operation. Table 4 summarizes the input power - output voltage relationship for the Model 1600XP depending on the range of selection. [Ref. 19: pp. 1-8]

Table 4. MODEL 1600XP WAVEFORM ANALYZER RANGE SETTINGS [From Ref. 19: p. 8]

PEAK INPUT POWER	RANGE SETTING	OUTPUT VOLTAGE
.1 μW to 10 μW	100 mV/μW	10 mV to 1 V
1 μW to 100 μW	10 mV/μW	10 mV to 1 V
10 μW to 1 mW	1 mV/μW	10 mV to 1 V

41

From Table 4, we observe that the input optical power given in microwatts can be determined from the measured output voltage level. If we desire to reference this input power to 1 milliwatt (1 mW), we can convert to the more conventional power units of dBm by using the following equation:

$$dBm = 10 \times \log_{10} \left[\frac{output\ voltage\ (V)}{range\ setting} \right]. \qquad (12)$$

For example, suppose the measured output voltage was 664 mV for a range setting of 10 mV/μW. The input optical power in dBm would be given by the expression $10 \times \log_{10}(0.664 \text{ V} \div 10 \text{ mV}/\mu\text{W})$; which is -11.78 dBm.

6. Power Budget

The prototype design of our network, as shown in Figure 9 on page 29, was used as the first iteration model for calculating a power budget. The following assumptions were made regarding the calculation of the power budget:

1. each 2x2 coupler (includes $n \times n$ star coupler, with $n = 2$) perfectly splits the input power in half causing equal amounts of power to exit on each delay line,

2. the total sum of all losses due to connectors is 4 dB,

3. fiber attenuation losses (dB/km) are negligible due to the short lengths of fiber used, and

4. other losses such as due to Fresnel reflection losses, misalignment effects, numerical aperture differences, and possibly index profile effects were determined to be small as compared to coupling losses.

Using the guidelines of the above assumptions, the total loss from transmitter to receiver (detector) due to splitting losses is 15 dB for the main lobe (or spike) of the autocorrelation waveform and at least 18 dB for all other lobes (sidelobes) of the autocorrelation waveform. As previously mentioned, the first four splitters are used to create the specific OOC. This creates a loss of about 12 dB (3 dB per splitter). The additional 3 dB loss, which gives a total loss of 15 dB, is generated by the 2x2 star coupler as it splits equal amounts of power between the two receivers. No further coupling losses occur to the subsequent main lobe as pulses are overlaid upon each other during the second pass through the series couplers. This phenomenon will be discussed further in the next two chapters. When we add in the assumed connector losses of 4 dB, the total loss to the autocorrelation peak is 19 dB, and the total loss to any other side peak of the autocorrelation function is 22 dB or greater. The autocorrelation peak in parallel networks has previously been shown to experience a loss of 25 dB using similar assumptions.

Our ultimate goal was to be able to detect the peak of the autocorrelation function. As mentioned above, the autocorrelation peak experiences a 19 dB power reduction due to coupling and connector losses. These losses represent a 6 dB improvement (factor of four) over a parallel coding approach. Using a laser diode as our source, we easily ensure ourselves of launching sufficient power into the fiber to be able to detect a data-pulse. We must, however, be aware that with the increased optical power falling on the receiver that overdriving the receiver is a

distinct possibility. An optical attenuator or a variable-gain receiver could be used to overcome this problem.

IV. ENCODER

A. DESIGN

The origin of our encoder must begin with the required code sequence, i.e., the OOC, which must be produced prior to entering the star coupler and being distributed throughout the network. Table 5 below illustrates Table 2 information in a slightly different manner in order to emphasize the delays required to achieve proper placement of the pulses. We recall that placement of all the pulses must be at integer multiples of the chip time.

Table 5. GRAPHICAL REPRESENTATION OF DESIRED CODE SEQUENCES.

g(2,4)													
X	1	0	0	1	0	0	0	0	0	0	0	0	1	1
Y	1	0	0	0	0	1	0	1	0	0	0	1	0	0
mult. of T_c	0	1	2	3	4	5	6	7	8	9	10	11	12	13

Table 6 is a graphical representation of the actual code sequences that were achieved with the ladder encoder. Each of the actual code sequences have four additional pulses within the complete code sequence. We will refer to these additional pulses as *redundant pulses*. Redundant pulses are a result of using a ladder network (serial

45

approach) vice a parallel approach to generate the code sequences. We will talk about the inherent problems resulting from the existence of the redundant pulses later in the chapter.

Table 6. GRAPHICAL REPRESENTATION OF ACTUAL CODE SEQUENCES.

mult. of T_c	0	1	2	3	4	5	6	7	8	9	10	11	12	13
X	1	0	0	1	0	0	0	0	0	1	0	0	1	1
Y	1	0	1	0	0	1	0	1	0	0	0	1	0	1

mult. of T_c	14	15	16	17	18	19	20	21	22	23	24	25
X	0	0	1	0	0	0	0	0	1	0	0	1
Y	0	0	1	0	1	0	0	0	0	0	0	0

In order to determine the length of fiber needed to impose delays which are a multiple of the chip time, we need to calculate the speed of light in the fiber material. Employing silica glass as the fiber material, having an index of refraction (n) equal to 1.47, we calculate the speed of light (v) in the fiber using the following relationship:

$$v = \frac{c}{n} = \frac{3 \times 10^8}{1.47} = 2.04 \times 10^8 \ m/s. \tag{13}$$

We can now calculate the required length of fiber required to impose a delay of one chip interval using the calculated value of the speed of light in silica and the known value of the pulse width.

$$length = (2.04 \times 10^8 \ m/s) \times (pulse \ width). \tag{14}$$

Table 7 provides a ready reference of calculated fiber lengths required to impose delays that are multiples of the chip time for several different pulse widths. One immediately notices how unwieldy the fiber lengths become as the chosen source pulse width increases. Neglecting the requirements to meet certain network data rates, one would choose the shortest possible source pulse width (chip time) in order to minimize the required lengths of fiber for each of the delay lines.

As previously mentioned, a 10 ns pulse width was chosen to be utilized for network implementation. This fixes the required delay line lengths for a specified OOC. Table 8 summarizes the required delay line lengths for both users given a 10 ns pulse width. Note that the lengths referred to are those lengths between couplers as specified by Figure 9 on page 29. A delay line length equal to zero represents a direct connection between splitters. To calculate the delay line lengths between couplers, one takes the difference between required pulse positions (required delay), enters Table 7 for this required delay and reads off the value under the 10 ns pulse width column. For example, if a pulse is required at position 1 and at position 7, the required delay line length would be 12.245 m.

Table 7. CALCULATED DELAY LINE LENGTHS (METERS).

	- Pulse Width -				
Required delay # T_c	10 ns	20 ns	30 ns	40 ns	50 ns
0	0	0	0	0	0
1	2.041	4.082	6.122	8.163	10.204
2	4.082	8.163	12.245	16.327	20.408
3	6.122	12.245	18.367	24.490	30.612
4	8.163	16.327	24.490	32.653	40.816
5	10.204	20.408	30.612	40.816	51.020
6	12.245	24.490	36.735	48.980	61.224
7	14.286	28.571	42.857	57.143	71.429
8	16.327	32.653	48.980	65.306	81.633
9	18.367	36.735	55.102	73.469	91.837
10	20.408	40.816	61.224	81.633	102.040
11	22.449	44.898	67.347	89.796	112.245
12	24.490	48.980	73.469	97.959	122.450
13	26.531	53.061	79.592	106.12	132.655

B. ENCODER IMPLEMENTATION

We began our construction of the encoder by cutting each delay line to the specified length in Table 8. It was stipulated that each delay line length could not vary more than 5% from specification. This was to ensure proper pulse placement within the chip period. Once the delay lines were of proper length, an AMP Incorporated Optimate 2.5 mm bayonet stainless steel connector (ST™ compatible)

48

Table 8. ENCODER DELAY LINE LENGTHS.

g(2,4)	User #1	User #2
Pulse number	Length (meters)	Length (meters)
1	L=0	L=0
2	L1a=6.122	L2a=10.204
3	L1b=18.367	L2b=4.082
4	L1c=26.531	L2c=22.449

was attached to each fiber end. The fiber ends were then carefully polished and inspected to ensure uniform performance. The delay lines were placed in the proper order and connected to the 2x2 couplers in a ladder (series) configuration. The network was then tested with the TEK TFP2 Fibermaster OTDR using a 10 ns pulse with a wavelength of 1550 nm. Figures 12-15 illustrate the progression of the construction of the OOC for user #1. Figure 12 documents the first pulse placement during the first chip period (0-10 ns) as it arrives at the detector. A replica of this pulse, but at half the initial power, exits the first splitter on each delay line. The pulses on the two delay lines arrive at the second splitter at different times due to the delay imposed on line L1a. Now two pulses exit the second splitter on each delay line at the first two required pulse positions in the OOC; the first chip interval (0-10 ns) and the fourth chip interval (30-40 ns) as noted in Figure 13. Once again due to
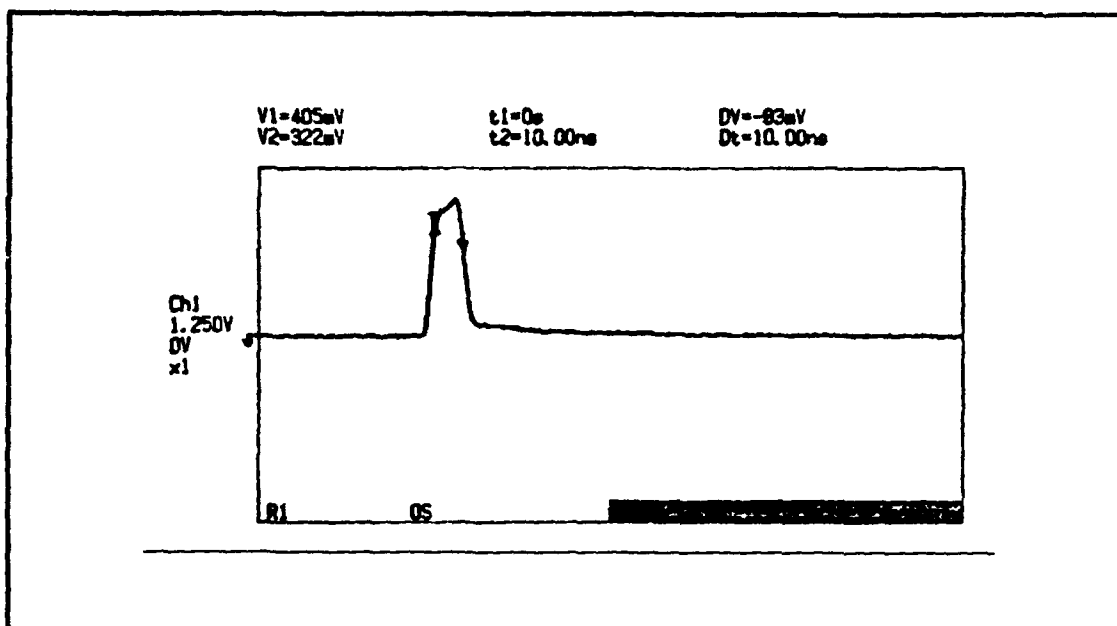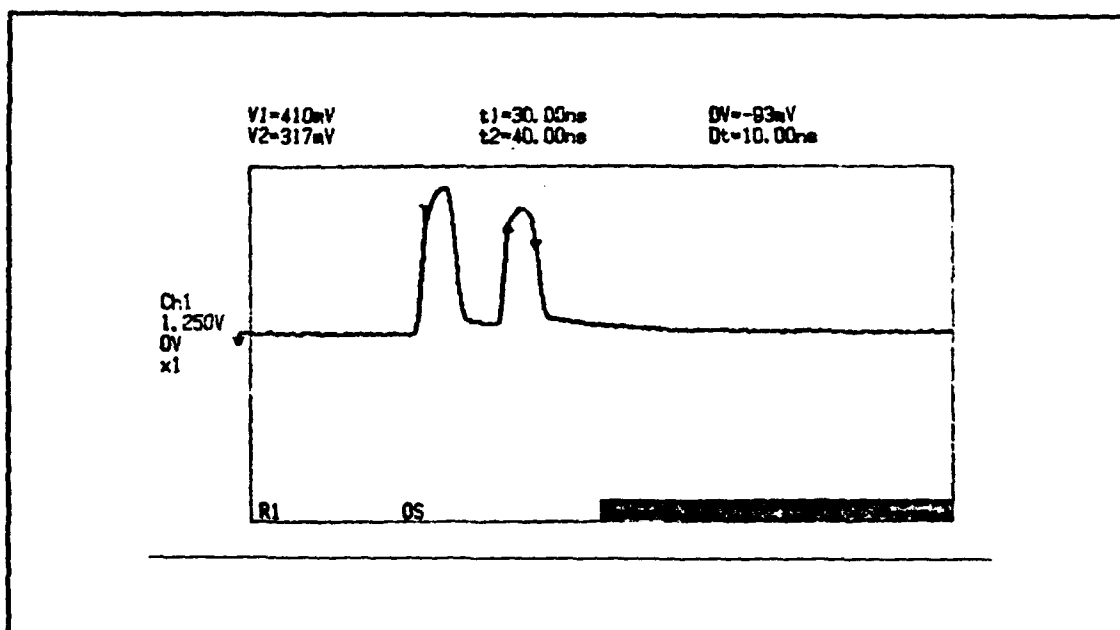
Figure 12. Pulse exiting first splitter.

Figure 13. Pulses exiting second splitter.

the imposed delay, this time due to delay line L2b, the two pairs of pulses arrive at

the third sp''' ter at predetermined times in order to generate the third pulse required

by the OOC. The pulse pairs are combined and exit the splitter as a four-pulse

Figure 14. Pulses exiting third splitter.

Figure 15. Pulses exiting fourth splitter (encoded signal).

sequence. Three of these pulses are desired: the pulses located at 0-10 ns, 30-40 ns, and 120-130 ns, as seen in Figure 14. The fourth pulse located in the tenth chip interval (90-100 ns) is one the redundant pulses we alluded to earlier. This pulse is

a result of delaying the first pulse nine chip intervals as the third pulse was generated from the second pulse by delaying the second pulse nine chip intervals. The redundant pulse is not desired but cannot be prevented from occurring since all pulses are generated in pairs (2x2 splitters). The fourth pulse we desire (130-140 ns) is shown in Figure 15. This pulse is a result of the delay imposed by delay line L1c and the combining of eight pulses, four pulses from each delay line. Figure 15 clearly shows the four desired pulses along with the four redundant pulses which were created.

The pulses we generated to form the code for user #1 were all within 80 mV of the average value of 550 mV/pulse (within 1.35 dB). This is highly desirable because if too much variance in the pulse magnitudes results, the ratio of the peak of the autocorrelation function to the peak of the maximum side lobe amplitude will be too small to ensure accurate detection results.

Figure 16 is the sequence generated for user #2. The four desired pulses have been labeled numbers 1-4. The other pulses are the redundant pulses. One immediately notices that the pulse magnitudes are not as uniform as they were for user #1. The result, as will be seen in Chapter VI, is a less than desirable autocorrelation function.

The main reason for the lack of uniformity among pulses was due to the different type of connectors utilized in constructing the ladder network for user #2. The SMA-style connectors were used instead of the ST-style connectors because the remaining 2x2 couplers on hand were already fitted with these connectors by the

manufacturer. Even though they were not the ideal first choice, significant resources were conserved by not purchasing additional couplers. The SMA connectors are widely used; however, they do not provide as reproducible a connection as ST-style connectors do. Thus if a network requires frequent assembly/disassemble, results may vary from time to time if connectors with less stringent specifications are used. Time and cost prevented the changing out of connectors for user #2.
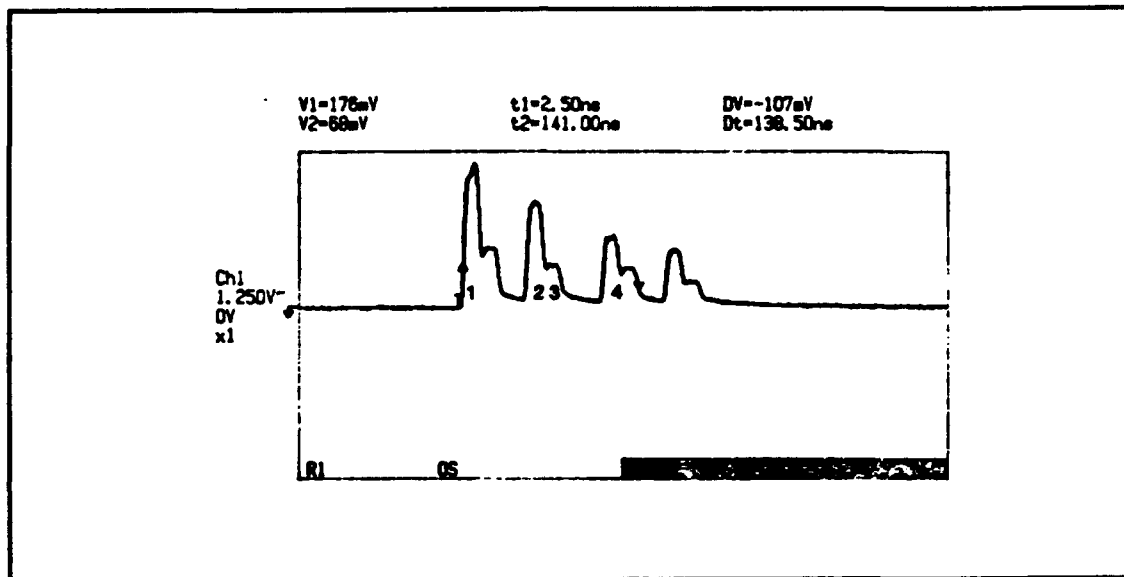

Figure 16. User #2 code sequence.

V. DECODERS

A. DESIGN

The design of our decoder is identical to our encoder design. This is because the same hardware is used for both encoding/decoding functions. This fact is what makes this network unique and cost effective. The idealized generated pulse sequence exiting the encoder and entering the decoder for user #1 is given by Figure 17. Figure 18 illustrates the ideal generated code sequence for user #2. These are the same pulse sequences which were used to generate the autocorrelation and cross-correlation functions in the computer program displayed in the Appendix. Hence, the computer generated outputs would be the ideal response of our design.
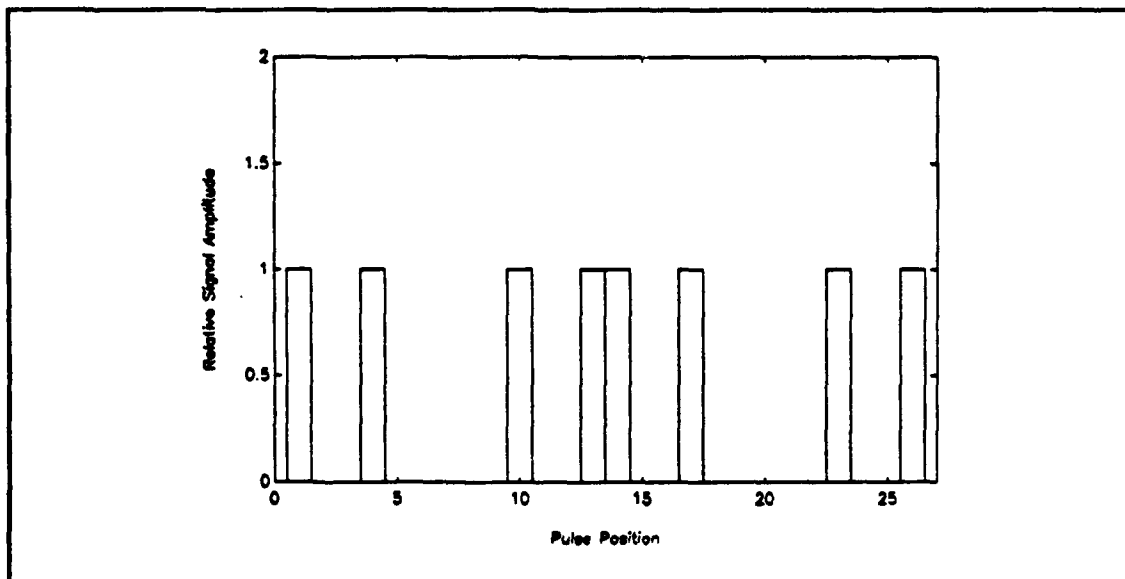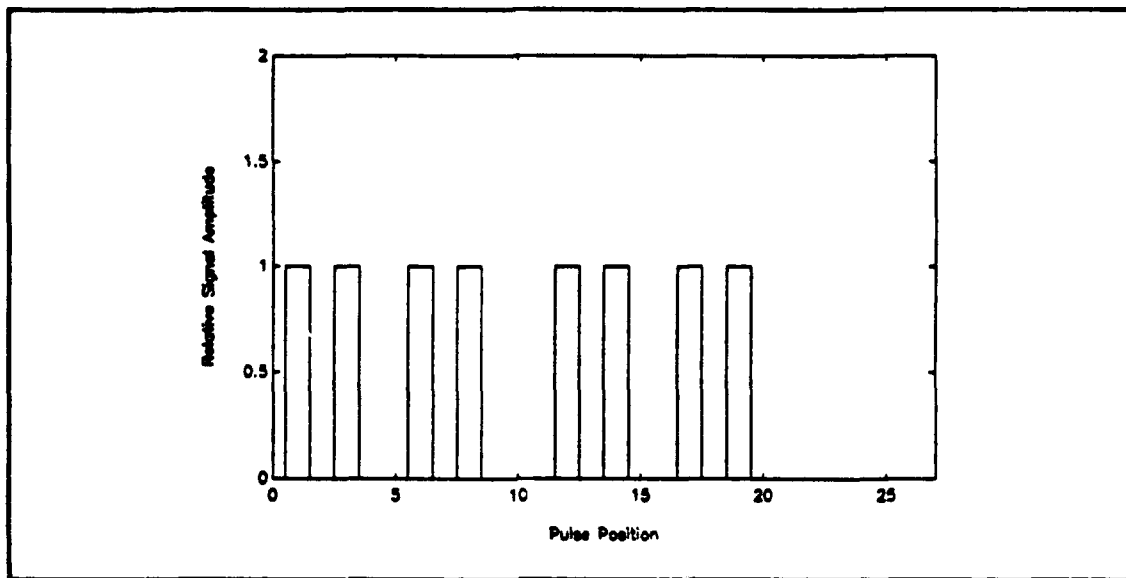

Figure 17. User #1 encoded signal.

Figure 18. User #2 encoded signal.

As the encoded signals are sent back through the series couplers, the pulses are appropriately delayed and combined such that at the decoder output the autocorrelation function results for the intended message and the cross-correlation function results for any interfering signals (the other user in our design). Figures 19 and 20 illustrate the matched filter response of the decoders for user #1 and user #2, respectively when the idealized generated code sequences shown in Figures 17 and 18 are sent through the intended decoder. Referring to Figures 19 and 20, we observe that the ratio of the peak value of the autocorrelation function to the peak value of the side lobes is only two rather than four. This demonstrates the negative effect of the redundant pulses. In previous designs using parallel networks, a ratio of four resulted between the peak of the autocorrelation function and the peak of the side lobes. This reduction by a factor of two is caused by the redundant pulses as they are delayed and overlaid on other pulses during the decoding process just as we

55
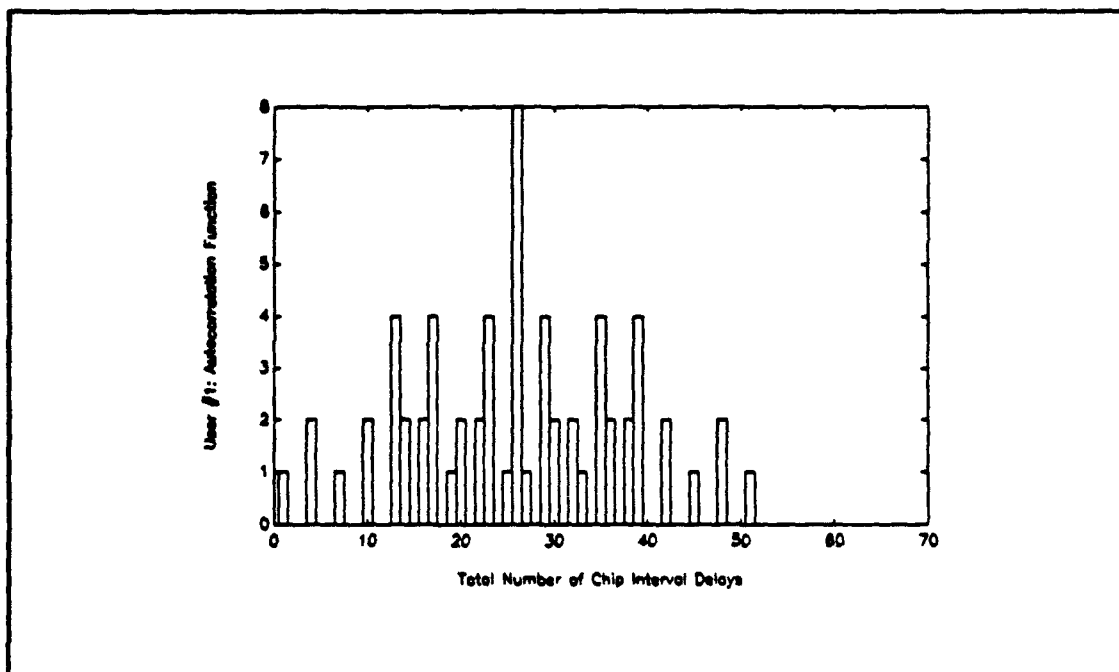
Figure 19. Autocorrelation function for User #1.
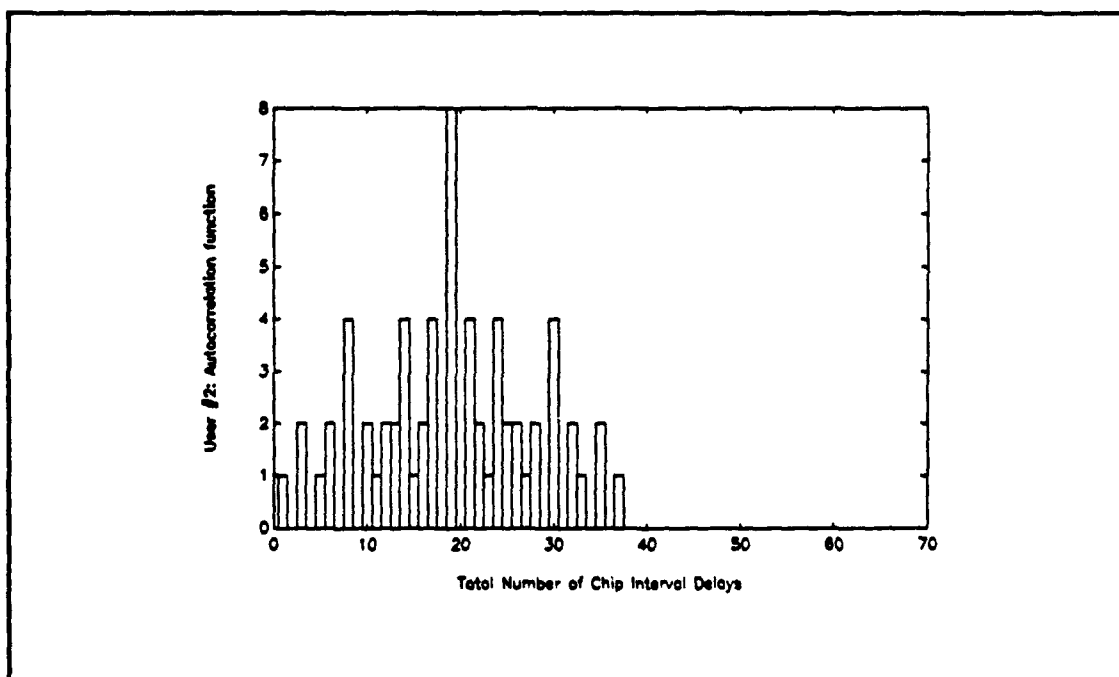
Figure 20. Autocorrelation function for User #2.

56

intend for the pulses of interest to undergo. This is one of the tradeoffs which must be made in choosing whether to utilize a series or a parallel network design.

Figure 21 demonstrates the system response (cross-correlation function) when encoded signal #1 is sent through the decoder of user #2. The identical response
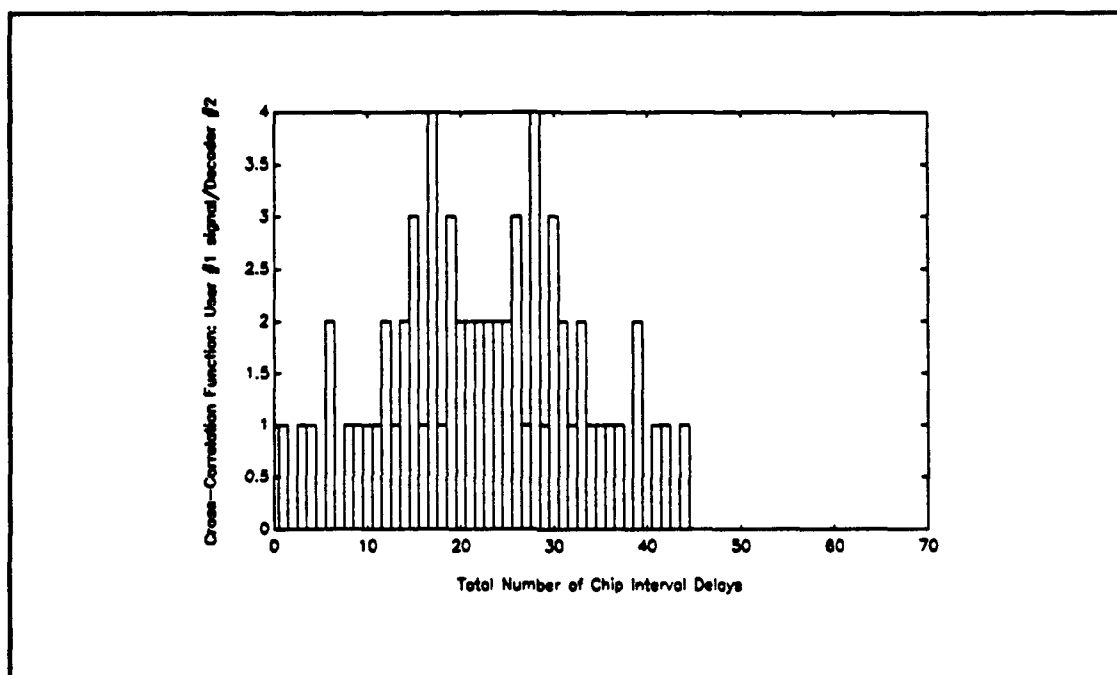

Figure 21. Cross-correlation function of User #1 with decoder #2.

occurs when encoded signal #2 is sent through the decoder of user #1. Two peaks are readily apparent when the cross-correlation function is observed. When the size of these peaks are compared to the size of the autocorrelation peak, we notice that a factor of two (which is the same as the ratio of the peak of the autocorrelation function to the peak value of the side lobes) results. A threshold type detector with an appropriately set trigger value would therefore prevent interfering signals or side lobes of intended signals to cause a false detection.

The final feature of our network design which must be addressed is the performance of the decoder when an interfering signal is present and is in perfect synchronization with the intended signal. Figure 22 illustrates the ideal response of the decoder for user #1 during simultaneous message transmission. Figure 23 is the ideal response of the decoder for user #2, also under the conditions of simultaneous message transmission.
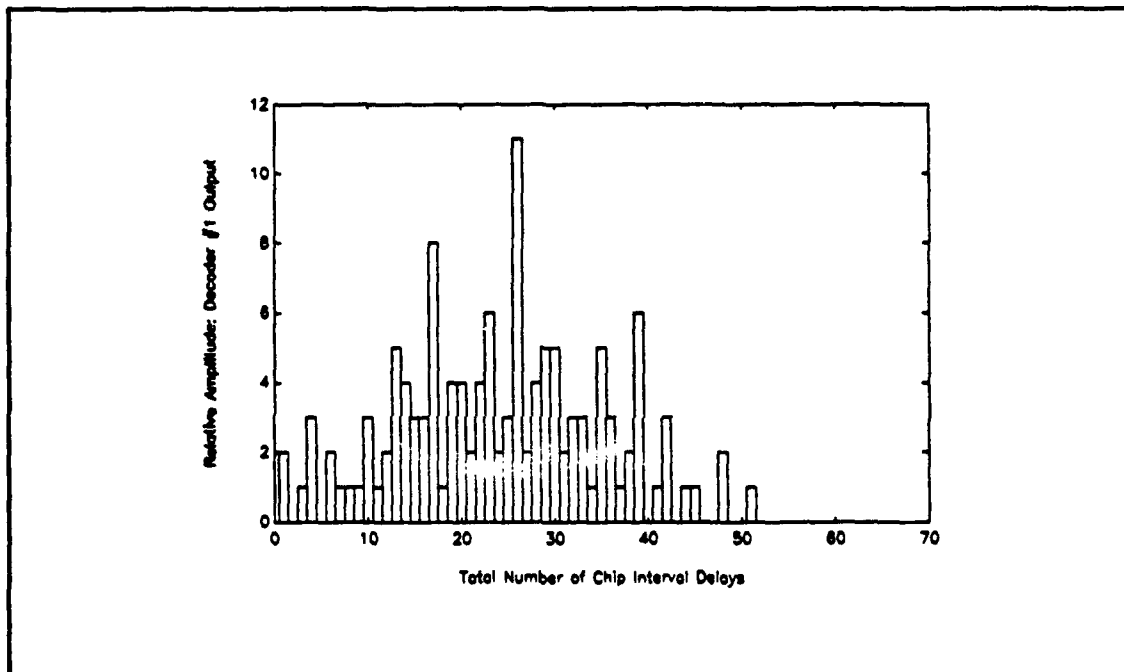

Figure 22. Decoder #1 response with simultaneous message transmission.

As we examine these figures, it is immediately apparent that the peak of both decoder responses occurs at the same time as they occurred in the single transmission case. The peak, however, is greater in magnitude. It is also evident that the side lobes

58

are also greater in magnitude as well as no longer being symmetric. These effects result in the ratio of the peak detector response to the peak side lobe value as no
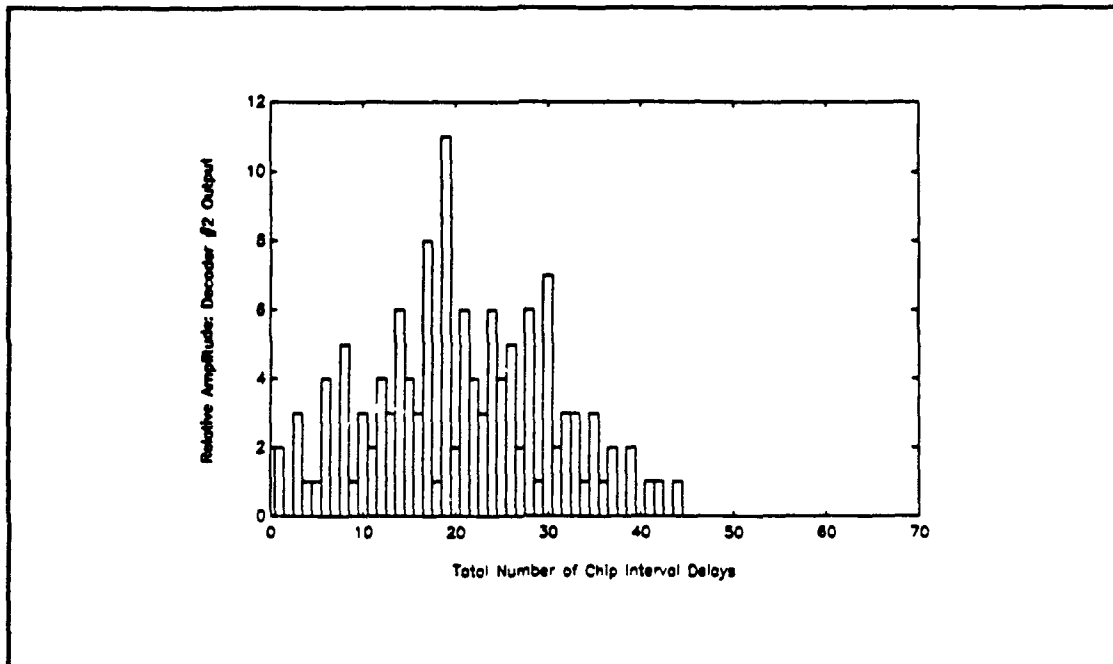

Figure 23. Decoder #2 response with simultaneous message transmission.

longer being two. To overcome the possible consequences of these phenomena we must respond in one of several different ways. We could design our detector with a variable threshold such that during simultaneous operations the threshold would be set at a higher value. This not only would be very expensive but would contradict one of our design goals of economical design. We could synchronize the detector with the message transmission such that the matched filter output would be sampled at the autocorrelation peak ensuring discrimination against the side lobes. However synchronization is contrary to our design specifications as well. The strategy chosen was to proceed with our original design and original specifications which allow

asynchronous access. Significant degradation in the intended decoder response will not occur. This is due to the fact that when the interfering signal is a "1" and the intended signal is a "0", the decoder output would be below the detectors threshold and would result in a "0" being received (refer to the discussion on the cross-correlation function). If the intended signal is a "1" and the interfering signal is a "1" or a "0", the threshold of the detector will be exceeded resulting in a "1" being received. In all cases the output of the detector is the same as the intended signal which is as desired.

In the final chapter we will demonstrate the actual performance of our network design.

VI. RESULTS/CONCLUSIONS

A. AUTOCORRELATION

To demonstrate the actual performance of our circuit under single-transmission conditions, the encoded signals displayed in Figures 15 and 16 on pages 50 and 52, respectively, were passed through their respective decoders at separate times with their autocorrelation functions being displayed on the Tektronix transient digitizer. The autocorrelation function for user #1 is displayed in Figure 24 and the
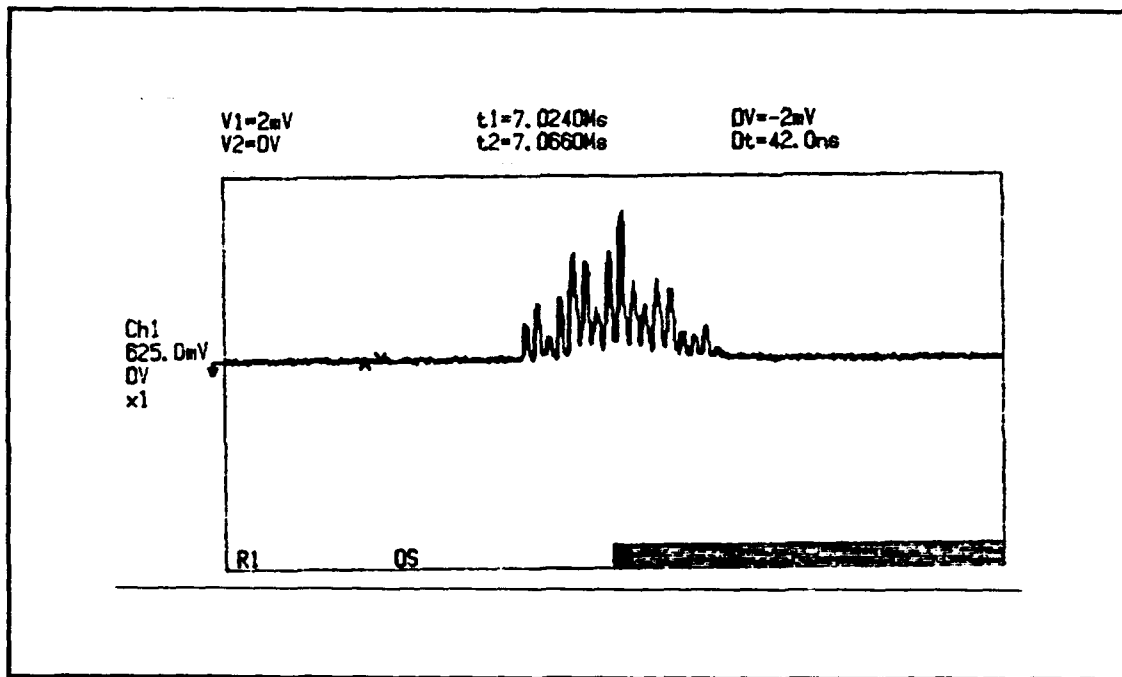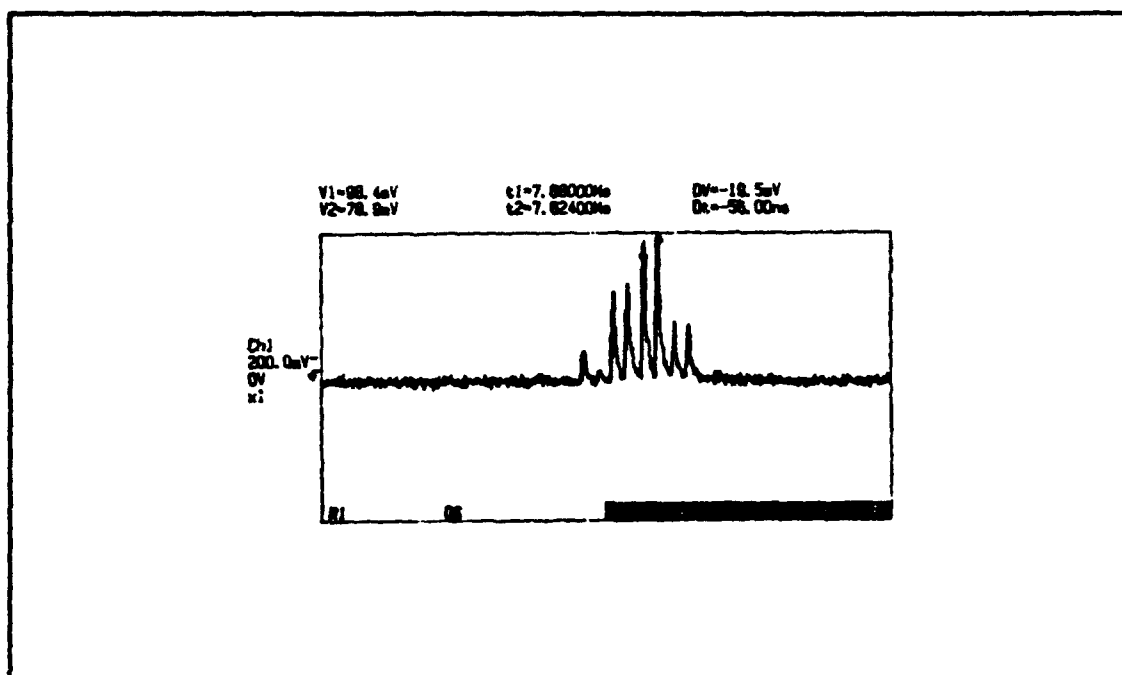

Figure 24. Autocorrelation function waveform for User #1.

autocorrelation function for user #2 is displayed in Figure 25. As we refer to these figures, we notice that the autocorrelation function for user #1 is more symmetric

Figure 25. Autocorrelation function waveform for User #2.

than for user #2. Additionally, the ratio of the peak value of the autocorrelation function to the peak side lobe value is also greater (as is desired) for user #1. The preferred characteristics found for user #1 are a result of achieving a uniform power distribution between the OOC pulses.

The goal of being able to set a specific threshold which discriminates against the autocorrelation functions side lobes while detecting the center autocorrelation peak was achieved. To illustrate this, the cursors in Figure 25 have been placed so that we can calculate the power ratio between the central peak and the maximum valued side lobe for user #2. The voltage ratio is calculated to be 98.4 mV/78.9 mV = 1.25 mV/mV. Since power is proportional to the square of the voltage, the power ratio is $(1.25 \text{ mV})^2$ which is approximately 1.56 W/W. This is slightly less than the

desired ratio of 2 W/W which would have resulted if our generated OOC was uniformly balanced in power. Even with this less than ideal performance, accurate detection can be achieved.

B. USER INTERFERENCE

Another goal in our design was to be able to discriminate against cross-talk (other user interference) to ensure false detections do not result in this instance. Figure 26 is the output of detector #2 with user #1 transmitting and user #2 idle.
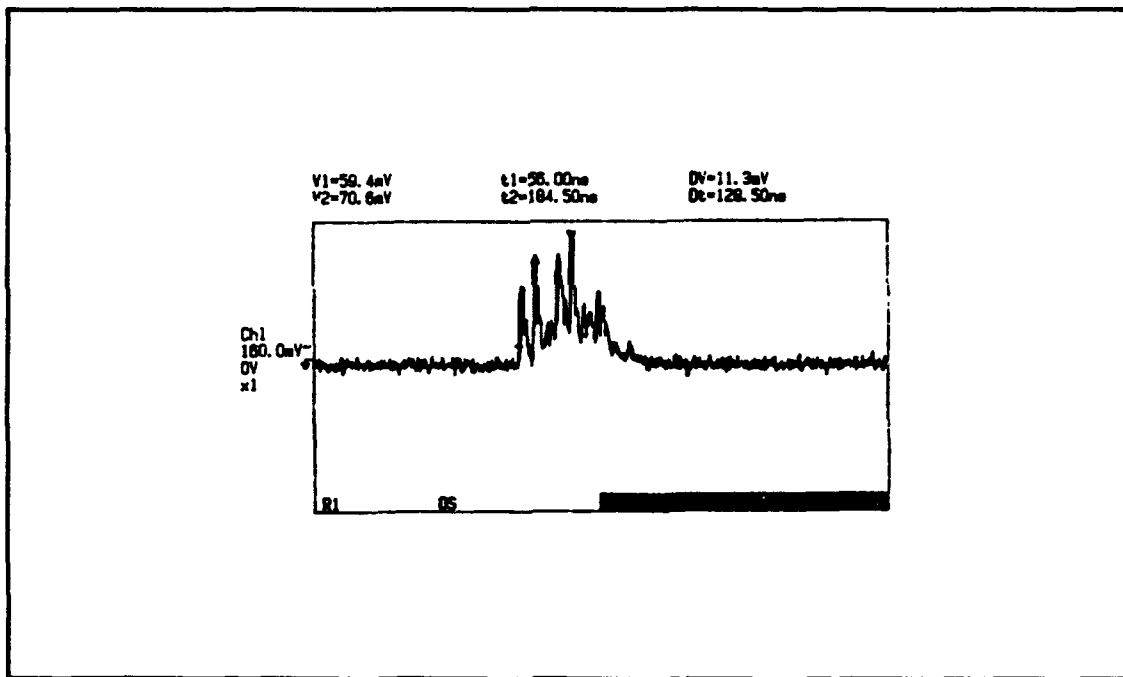

Figure 26. Cross-correlation function: User #1 transmitting/User #2 idle.

This represents a cross-correlation function. Our requirement with the cross-correlation function is that the largest peak is sufficiently less than the

autocorrelation peak such that they can be distinguished from one another by a threshold detector.

As we refer to Figure 26, the largest peak has been measured at a value of 70.6 mV. This value is less than the peak side lobe value indicated in Figure 25 as 78.9 mV. This being the case, any threshold value which ensures discrimination against the largest side lobe also satisfactorily rejects the maximum cross-talk value. Hence we are ensured of acceptable performance during asynchronous access when no users are simultaneously transmitting.

C. SIMULTANEOUS TRANSMISSION

A preliminary investigation in the case of simultaneous transmissions has been initiated. Conclusive results have not yet been attained; however network performance is certainly degraded when multiple transmissions are perfectly synchronized as we saw in chapter five in our theoretically generated data.

Perfect synchronization of multiple optical sources in the laboratory is difficult to achieve. As a result, to attain synchronization of both users signals, one source was used to generate a signal in both ladder networks at the identical time. To accomplish this feat, an additional 2x2 splitter was added to the network such that the output of the OTDR was split sending a pulse into both networks simultaneously. Another 2x2 splitter was added to combine the encoded signals of user #1 and user #2 with the combined signal being passed through the decoder side of user #2. As a result, the autocorrelation of user #2 was performed in the presence of

64
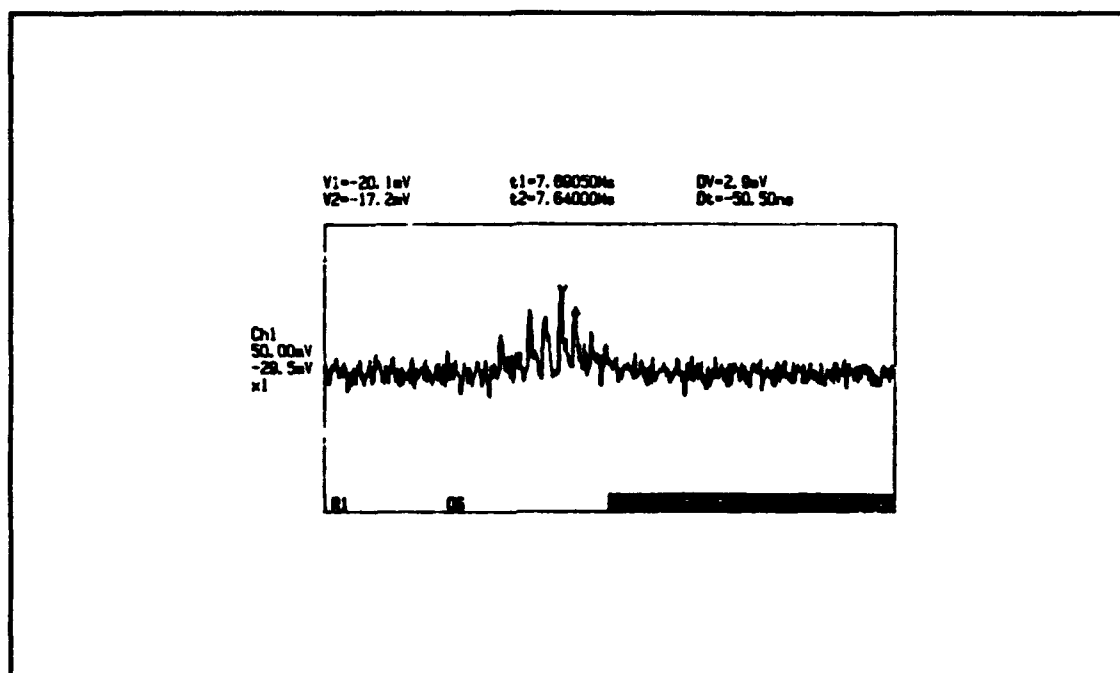
Figure 27. Simultaneous transmission by both users.

interference from user #1. Figure 27 displays the results of simultaneous transmission. The major difficulty of making firm conclusions from this display is the fact that an additional factor of four in power reduction occurred as a result of the newly added 2x2 splitters. This power reduction has resulted in some of the expected pulses to drop within the noise level and to no longer be distinguishable. Even though a peak pulse can be discerned from the others, not enough information is available to conclude if this indeed corresponds to the intended autocorrelation peak or if it is one of the interfering pulses. Further research in the effects of simultaneous cross-talk must continue in order to establish firm conclusions.

D. CONCLUSIONS

This research represents the prototype design of an all-optical signal processing CDMA two-user local area network. This data link was designed, built, and tested with successful results. Modified optical orthogonal code sequences (OOCs) were generated by serially connecting 2x2 couplers and delay lines. Through the use of a serial network (as opposed to a parallel network) we were able to reduce network costs by using fewer couplers. This series design also resulted in a 6 dB power advantage over previous designs.

We demonstrated that proper selection of the chosen detectors threshold would result in accurate detection of intended signals while rejecting (discriminating against) interfering signals under the single transmission assumption. Even though in certain networks (low duty cycle, bursty traffic) simultaneous transmissions are unlikely, our network specifications did not stipulate any signal transmission characteristics other than data rate. This necessitated our commencement of research in the area of cross-talk. This research has yet to be taken to its conclusion but is definitely a driving factor on the capacity of future expanded networks.

APPENDIX

The following MATLAB source code was written to generate the code sequences for User #1 and User #2. These source codes were also used to produce the autocorrelation function and cross-correlation function for both users. Once the required data was available, the effects of cross-talk and simultaneous transmission could be simulated as well.

A.   MATLAB SOURCE CODE

```
clg
clear                     % generation of encoded signal for user #1
for i=1:1:60
        if i= =1
            a(i)=1;
        else
            a(i)=0;
        end
end
b=[0,0,0,a];
bb=b(1:60)+a;
c=[0,0,0,0,0,0,0,0,0,bb];
cc=c(1:60)+bb;
d=[0,0,0,0,0,0,0,0,0,0,0,0,0,cc];
dd=d(1:60)+cc;           % dd is the encoded signal of user #1

% bar(dd(1:14))          % pulse at dd(10) is a result of using ladder to encode
pause                    % i.e. gives redundant pulse

e=[0,0,0,dd];            % decoding signal of user #1
ee=e(1:60)+dd;
f=[0,0,0,0,0,0,0,0,0,ee];
ff=f(1:60)+ee;
g=[0,0,0,0,0,0,0,0,0,0,0,  0,0,ff];
gg=g(1:60)+ff;           % gg is the decoded signal of user #1

% plot(gg)               % graph of the autocorrelation of user #1's signal
% meta cdma
pause
bar(gg)                  % graph of the autocorrelation of user #1's signal
```

```
                              % in form of bar graph
ylabel('User #1: Autocorrelation Function')
xlabel('Total Number of Chip Interval Delays')
meta cdma11
pause
gg;                           % gives numerical values for autocorrelation of user #1's
                              % signal


for j=1:1:60                  % generation of encoded signal for user #2
      if j==1
          a2(j)=1;
      else
          a2(j)=0;
      end
end
b2=[0,0,0,0,0,a2];
bb2=b2(1:60)+a2;
c2=[0,0,bb2];
cc2=c2(1:60)+bb2;
d2=[0,0,0,0,0,0,0,0,0,0,0,0,cc2];
dd2=d2(1:60)+cc2;             % dd2 is the encoded signal of user #2


% bar(dd2(1:14))              % pulse at dd2() is a result of using ladder to encode
pause                         % i.e. gives redundant pulse


e2=[0,0,0,0,0,dd2];           % decoding signal of user #2
ee2=e2(1:60)+dd2;
f2=[0,0,ee2];
ff2=f2(1:60)+ee2;
g2=[0,0,0,0,0,0,0,0,0,0,0,0,ff2];
gg2=g2(1:60)+ff2;            % gg2 is the decoded signal of user #2


% plot(gg2)                   % graph of the autocorrelation of user #2's signal
% meta
pause
bar(gg2)                      % graph of the autocorrelation of user #2's signal
                              % in bar graph form
ylabel('User #2 Autocorrelation Function')
xlabel('Total Number of Chip Interval Delays')
meta cdma 22
pause
gg2;                          % numerical values for autocorrelation of user #2's signal
```

68

```
e22 = [0,0,0,0,0,dd];          % Cross-correlation using encoded signal #1 with receiver
                               % (decoder) #2

ee22 = e22(1:60) + dd;
f22 = [0,0,ee22];
ff22 = f22(1:60) + ee22;
g22 = [0,0,0,0,0,0,0,0,0,0,0,ff22];
gg22 = g22(1:60) + ff22;


e11 = [0,0,0,dd2];             % Cross-correlation using encoded signal #2 with receiver
                               % (decoder) #1

ee11 = e11(1:60) + dd2;
f11 = [0,0,0,0,0,0,0,0,0,ee11];
ff11 = f11(1:60) + ee11;
g11 = [0,0,0,0,0,0,0,0,0,0,0,0,ff11];
gg11 = g11(1:60) + ff11;


clg
bar(gg22)
ylabel('Cross-Correlation Function: User #1 signal/Decoder #2')
xlabel('Total Number of Chip Interval Delays')
meta cdma 12
pause


bar(gg11)
ylabel('Cross-Correlation Function: User #2 signal/Decoder #1')
xlabel('Total Number of Chip Interval Delays')
meta cdma21
pause


end
```

LIST OF REFERENCES

1. Rodger E. Ziemer and Roger L. Peterson, *Digital Communications and Spread Spectrum Systems*, Macmillan Publishing Company, New York, 1985.

2. J. P. Powers, *An Introduction to Fiber Optic Systems*, Aksen Associates and R. D. Irwin, Inc., Homewood, Illinois, 1993.

3. R. L. Pickholtz, D. L. Schilling, and L. B. Milstein, "Theory of Spread-Spectrum Communications - A Tutorial," *IEEE Trans. Comm.*, vol. COM-30, no. 5, pp. 855-884, May 1982.

4. L. W. Couch II, *Digital and Analog Communications Systems*, 3rd ed., Macmillan Publishing Company, New York, 1990.

5. D. L. Schilling, L. B. Milstein, R. L. Pickholtz, M. Kullback, and F. Miller, "Spread Spectrum for Commercial Communications," *IEEE Communications Magazine*, pp. 66-78, April 1991.

6. T. T. Ha, *Digital Satellite Communications*, 2nd ed., McGraw-Hill, Inc. Publishing Company, 1990.

7. J. A. Salehi and C. A. Bracket, "Fundamental Principles of Fiber Optic Code Division Multiple Access (FO-CDMA)," Proc. IEEE Int. Conf. Communications, Seattle, Washington, pp. 1601-1609, 1987.

8. John W. Andre, Lieutenant, United States Navy, "Feasibility Study of Implementing a Code Division Multiple Access Data Link Utilizing Fiber Optic Delay Lines," Naval Postgraduate School, Monterey, California, MSEE Thesis, September, 1992.

9. E. Marom, "Optical Delay Line Matched Filters," *IEEE Trans. Circ. Syst.*, CAS-25, no. 6, pp. 360-364, June 1978.

10. Robert C. Dixon, *Spread Spectrum Systems*, 2nd ed., John Wiley & Sons, Inc., 1984.

11. P. R. Prucnal, M. A. Santoro, "Spread Spectrum Fiber-Optic Local Area Network Using Optical Processing," *IEEE Journal of Lightwave Technology*, vol. LT-4, no. 5, pp. 547-554, May 1986.

12. S. Tamura, S. Nakano, and K. Okazaki, "Optical Code-Multiplex Transmission by Gold Sequences," *IEEE Journal of Lightwave Tech.*, vol. LT-3, no. 1, pp. 121-127, February 1985.

13. K. P. Jackson, S. A. Newton, B. Moslehi, M. Tur, C. C. Cutler, J. W. Goodman, and H. J. Shaw, "Optical Fiber Delay-Line Signal Processing," *IEEE Trans. Microwave Theory and Techniques*, vol. MTT-33, no. 3, pp. 193-210, March 1985.

14. M. E. Marhic, "Trends in Optical CDMA," OE/Fibers Conference, Boston, Massachusetts, September 8-9, 1992.

15. J. A. Salehi, "Code Division Multiple-Access Techniques in Optical Fiber Networks - Part I: Fundamental Principles," *IEEE Trans. on Communications*, vol. 37, no. 8, pp. 824-833, August 1989.

16. Farhad Khansefid, Herbert Taylor, and Robert Gagliardi, "Design of (0,1) Sequence Sets for Pulse Coded Systems," IEEE International Symposium on Information Theory, San Diego, California, January 14-19, 1990.

17. Tektronix, *TFP2 FiberMaster Optical Time Domain Reflectometer*, Operator Manual, Tektronix, Inc., 1991.

18. Tektronix, *RTD720A Transient Digitizer*, User Manual, Tektronix, Inc., 1992.

19. Photodyne, Inc., *Model 1600XP Waveform Analyzer*, Instruction Manual, Photodyne, Inc., 1984.

INITIAL DISTRIBUTION LIST

No. Copies

1. Defense Technical Information Center   2
   Cameron Station
   Alexandria, Virginia 22304-6145

2. Library, Code 52   2
   Naval Postgraduate School
   Monterey, California 93943-5101

3. Chairman, Code EC   1
   Department of Electrical and Computer Engineering
   Naval Postgraduate School
   Monterey, California 93943-5121

4. Professor John P. Powers, Code EC/Po   4
   Department of Electrical and Computer Engineering
   Naval Postgraduate School
   Monterey, California 93943-5121

5. Professor Alex W. Lam, Code EC/La   1
   Department of Electrical and Computer Engineering
   Naval Postgraduate School
   Monterey, California 93943-5121

6. Lieutenant Commander Bruce A. Legge, USN   1
   804 Bryan Street
   Normal, Illinois 61761